



Review article

Recent developments in solar-powered membrane distillation for sustainable desalination

Ahmad S. Jawed^{a,b,1}, Lobna Nassar^{a,c,1}, Hanaa M. Hegab^{a,b,*},
Riaan van der Merwe^c, Faisal Al Marzooqi^{a,b}, Fawzi Banat^{a,b}, Shadi W. Hasan^{a,b,**}

^a Center for Membranes and Advanced Water Technology (CMAT), Khalifa University of Science and Technology, PO Box, 127788, Abu Dhabi, United Arab Emirates

^b Department of Chemical and Petroleum Engineering, Khalifa University of Science and Technology, PO Box, 127788, Abu Dhabi, United Arab Emirates

^c Department of Civil Infrastructure and Environmental Engineering, Khalifa University of Science and Technology, PO Box, 127788, Abu Dhabi, United Arab Emirates

ARTICLE INFO

Keywords:

Desalination
Membrane technology
Photothermal membranes
Sustainable water treatment
Solar-powered membrane distillation

ABSTRACT

The freshwater shortage continues to be one of the greatest challenges affecting our planet. Although traditional membrane distillation (MD) can produce clean water regardless of climatic conditions, the process wastes a lot of energy. The technique of solar-powered membrane distillation (SPMD) has received a lot of interest in the past decade, thanks to the development of photothermal materials. SPMD is a promising replacement for the traditional MD based on fossil fuels, as it can prevent the harmful effects of emissions on the environment. Integrating green solar energy with MD can reduce the cost of the water purification process and secure freshwater production in remote areas. At this point, it is important to consider the most current progress of the SPMD system and highlight the challenges and prospects of this technology. Based on this, the background, recent advances, and principles of MD and SPMD, their configurations and mechanisms, fabrication methods, advantages, and current limitations are discussed. Detailed comparisons between SPMD and traditional MD, assessments of various standards for incorporating photothermal materials with desirable properties, discussions of desalination and other applications of SPMD and MD, and energy consumption rates are also covered. The final section addresses the potential of SPMD to outperform traditional desalination technology while improving water production without requiring a significant amount of electrical or high-grade thermal energy.

1. Introduction

Due to the growing population and fast industry development, the demand for potable water is persistently increasing and has

* Corresponding authors. Center for Membranes and Advanced Water Technology (CMAT), Khalifa University of Science and Technology, PO Box, 127788, Abu Dhabi, United Arab Emirates.

** Corresponding authors. Center for Membranes and Advanced Water Technology (CMAT), Khalifa University of Science and Technology, PO Box, 127788, Abu Dhabi, United Arab Emirates.

E-mail addresses: hanaa.hegab@ku.ac.ae (H.M. Hegab), shadi.hasan@ku.ac.ae (S.W. Hasan).

¹ These authors contributed equally to this work.

<https://doi.org/10.1016/j.heliyon.2024.e31656>

Received 19 December 2023; Received in revised form 2 April 2024; Accepted 20 May 2024

Available online 22 May 2024

2405-8440/© 2024 The Authors. Published by Elsevier Ltd. This is an open access article under the CC BY-NC license (<http://creativecommons.org/licenses/by-nc/4.0/>).

Nomenclature

AGMD	Air-gap membrane distillation
BP	Bucky paper
CA	Contact Angle
CB	Carbon black
CNT	Carbon-nanotubes
CVD	Chemical vapor deposition
DCMD	Direct-contact membrane distillation
DSMD	Direct solar membrane distillation
ESM	Egg-shell membrane
G	Graphene
GO	Graphene oxide
GOR	Gain-output ratio
LCA	Life cycle assessment
LEP	Liquid entry pressure
MED	Multi-effect distillation
MENA	Middle East and North Africa
MMM	Mixed matrix membrane
MOF	Metal-organic framework
MSF	Multi-stage flash
MWCNT	Multi-walled carbon nanotubes
NESMD	Nanophotonic enabled solar membrane distillation
NIPS	Non-solvent induced phase separation
NP	Nanoparticle
PDA	Polydopamine
PDMS	Polydimethylsiloxane
PMD	Photothermal Membrane Distillation
PP	Polypropylene
PTFE	Poly-tetra fluoroethylene
PV	Photovoltaic
PVDF	Polyvinylidene fluoride
r-GO	Reduced-Graphene oxide
RES	Renewable energy source
RO	Reverse Osmosis
SBS	Styrene-butadiene-styrene
SGMD	Sweeping-gas membrane distillation
SPMD	Solar powered membrane distillation
STD	Solar thermal distillation
TP	Temperature Polarization
VEDCMD	Vacuum enhanced direct contact membrane distillation
VMD	Vacuum membrane distillation

become one of the world's major challenges in the world [1–3]. For instance, regions such as the Middle East and North Africa (MENA) are the most water-scarce regions, with a rapidly growing rate of population, which urgently require inclusive steps to close the gap between high water demand and limited resource availability [4]. According to the United Nations World Water Development Report 2020 states that, a staggering 4.2 billion individuals lack proper sanitation facilities, while an additional 2.2 billion people continue to face the challenge of limited access to safe drinking water [5]. As a result, the worldwide desalination market is estimated to increase, coping with the growth of populations in Europe and the MENA by 74 % [6].

Desalination and wastewater treatment technologies can be considered feasible keys to tackling the challenge of water scarcity. Solar Powered Membrane Distillation (SPMD) with photothermal material-based membranes emerges as a highly promising desalination method. It offers the potential to utilize low-grade and renewable energy sources efficiently. In general, membrane distillation (MD) is a thermally induced membrane process wherein water evaporates at the membrane feed side, traverses through hydrophobic membrane pores, and, owing to the temperature disparity between the permeate and feed sides, ultimately condenses into freshwater on the colder permeation side [7]. Because of its exceptional properties, MD is a desired technology for lengthy separation operations.

The most intriguing component of MD technology is its ability to separate high-saline water efficiently. It is also used in the food, pharmaceutical, and environmental sectors. In addition, it can be used alone or as the last step in conjunction with other separation techniques [8]. Nevertheless, the commonly employed conventional MD (CMD) method presents significant drawbacks, including its reliance on a centralized and sizable pumping plant, inevitable heat loss during the transfer of feed from heating units to membrane

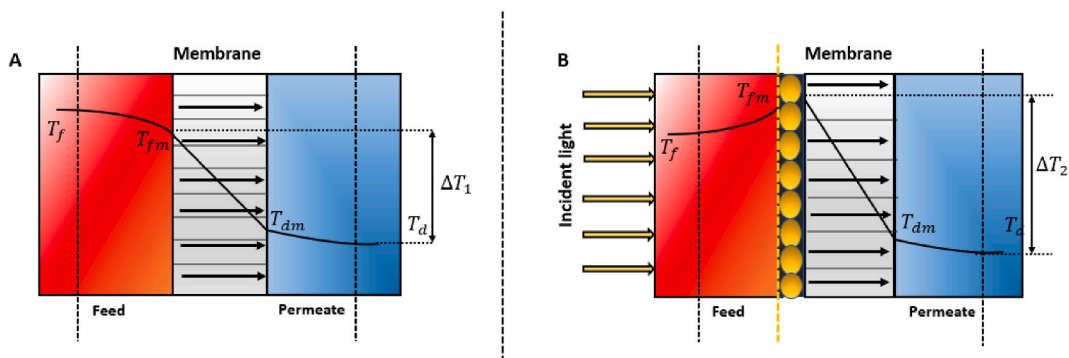


Fig. 1. Temperature profiles in (A) CMD and (B) SPMD configurations reflect the TP phenomenon.

modules, and elevated energy consumption for heating bulk feed water. On the other hand, the SPMD systems reduce the need for power generation systems and sophisticated equipment, offering a huge opportunity for developing highly portable and integrated devices for use in distant off-grid places. Furthermore, this approach mitigates heat loss during feed storage and transportation by delivering thermal energy directly to the photothermal layer of the membranes. This results in a significantly enhanced thermal energy efficiency, measuring at $60 \pm 10 \%$, in stark contrast to the below 10% thermal energy efficiency observed in CMD [9].

Another significant hurdle in the widespread adoption of CMD at a large scale is its diminished thermal efficiency, primarily attributed to temperature polarization. Temperature polarization (TP) is an inherent phenomenon resulting from conductive heat transport and the latent heat characteristics of the hydrophobic microporous membrane used in the process [10]. The thermal conductivity of the membrane and the process of water vaporization contribute to a lower temperature at the membrane surface feed interface (T_{fm}) compared to the temperature of the bulk feed water (T_f). Similarly, the temperature of the bulk distillate (T_d) is lower than that of the distillate membrane interface (T_{dm}). Consequently, TP significantly reduces the temperature differential at the membrane interface, in stark contrast to the theoretical driving force across the bulk phases as presented in Fig. 1A. To mitigate TP and enhance the performance of MD, researchers have explored various strategies, one of which is the incorporation of photothermal membranes. A photothermal membrane typically consists of a membrane material embedded with light-absorbing nanoparticles or coatings. When exposed to light, these materials efficiently convert light energy into heat, leading to localized heating at the membrane surface. By leveraging light-absorbing materials to generate localized heating at the membrane surface, photothermal membranes improve evaporation rates, reduce temperature gradients, increase mass transfer rates, and enable selective heating, thereby improving the efficiency and effectiveness of MD for various applications. As a result, the T_{fm} is higher than the T_f , and likewise, the T_d is higher than the T_{dm} (Fig. 1B).

Various technologies for mitigating the negative impacts of TP have been proposed in the literature, such as the use of modified feed channels [11] or feed spacers [12]. Nonetheless, the employment of these strategies increases the need for energy. The capacity to

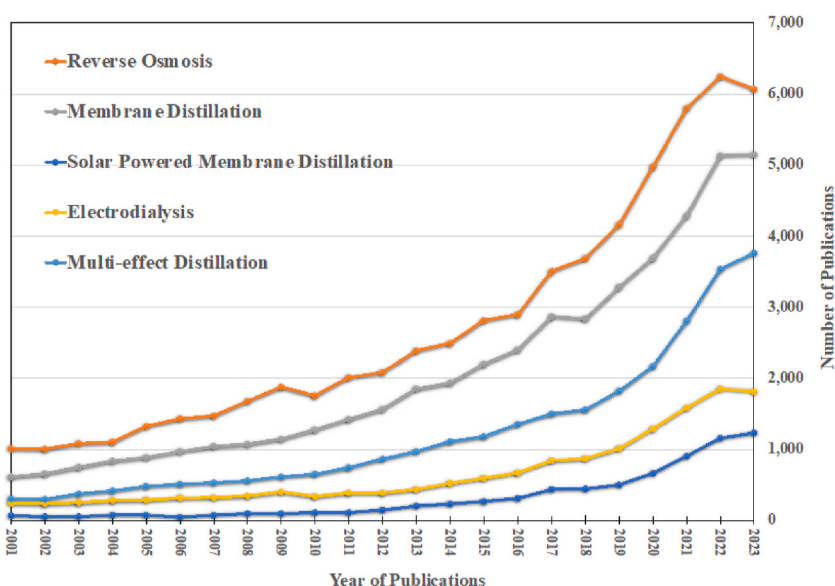


Fig. 2. Number of publications since 2000 by type of desalination technology (database obtained using ScienceDirect's advanced search system).

capture and utilize the kinetic energy of light for generating and controlling substantial heat at the nanoscale has led to the proposition of employing photothermal materials as nano heat sources in membranes. This innovative approach aims to address TP reduction, giving rise to a novel configuration referred to as photothermal membrane distillation (PMD) [13]. By inducing localized heat generation on the membrane surface and establishing a highly efficient transmembrane temperature gradient for vapor transportation, the process adeptly tackles challenges inherent in CMD processes, including TP, thermal losses, and energy-intensive operations. Moreover, it also experiences fewer occurrences of membrane fouling, requires lower power input, and involves reduced external heat input [9].

Reverse osmosis (RO) and MD are currently the dominant industrial technologies for seawater desalination applications [14,15], as demonstrated in Fig. 2. Nevertheless, those processes have some drawbacks and technical difficulties. There is still ongoing research to enhance the durability of membrane processes and reduce membrane costs. Moreover, one of the primary problems that contributes to the complexity and increased cost of such procedures is fouling. Additionally, they are considered energy-intensive, either by high-pressure demand (RO) or by heat demand (thermal processes), which generates undesired emissions and more pollutants. These drawbacks obstructed the economic viability of such procedures, necessitating the quest for eco-friendly and long-term desalination methods. The number of articles published, in the last 20 years, on solar energy for desalination has expanded dramatically, indicating a surge in interest in the field. However, it is still a relatively new research field when compared to other technologies. Therefore, more research is expected to be carried out in this new field to reduce greenhouse gas emissions and energy consumption.

Considering the recent substantial successes in the PMD process and its promising potential for decentralized desalination, it is necessary to conduct a full evaluation of PMD's recent progress, current condition, and possible prospects compared to the CMD. After the discussion of the MD state-of-the-art in the next section, Section 3 presents the SPMD technology in terms of mechanisms, module designs, pros, and cons. Section 4 illustrates the common membrane characteristics of both MD and SPMD, as well as the various approaches for their membrane fabrication. Each approach's strengths and limitations are highlighted. For simplicity, the membrane fabrication approaches were grouped into one- and multi-step. The following section describes the various fillers used in the MD and SPMD membranes, including carbon-based, metal oxide, and metals/metal-organic frameworks (MOFs) materials. Finally, the paper also presents the techno-economics, pilot studies, and future perspectives of SPMD technology to help with future studies. This comprehensive review aims to acquaint readers with the foundational principles and the present state of membrane distillation (MD) and SPMD technologies. The goal is to inspire and motivate a broader audience to engage in the development of efficient photothermal membranes for SPMD, to address the existing challenges that impede its widespread practical applications.

2. Is SPMD taking over CMD?

MD consumes a lot of energy based on fossil fuels. However, abundant, economical, and environment-friendly energy sources can be advantageous for MD. By utilizing low-grade heat sources, the MD technique can lower the amount of power used. Waste heat sources from industrial and power plants, low-temperature solar thermal collectors, and geothermal reservoirs are all low-grade heat sources being examined for the MD process [16]. Thermal desalination systems have inherent inefficiencies; thus, before using heat energy for other purposes, district heating for commercial and residential areas should be considered [17–19].

Low-grade heat sources from industrial sources would be more feasible, but there are no assessments of the amount and temperature of the heat already available [20]. Given that the MD method aids in lowering the discharge temperatures to protect receiving water systems and comply with standards, the use of waste heat in MD may further benefit the environment [21]. The design, installation, and testing of SPMD have been the subject of numerous research projects over the past 20 years. For example, Guillén et al.

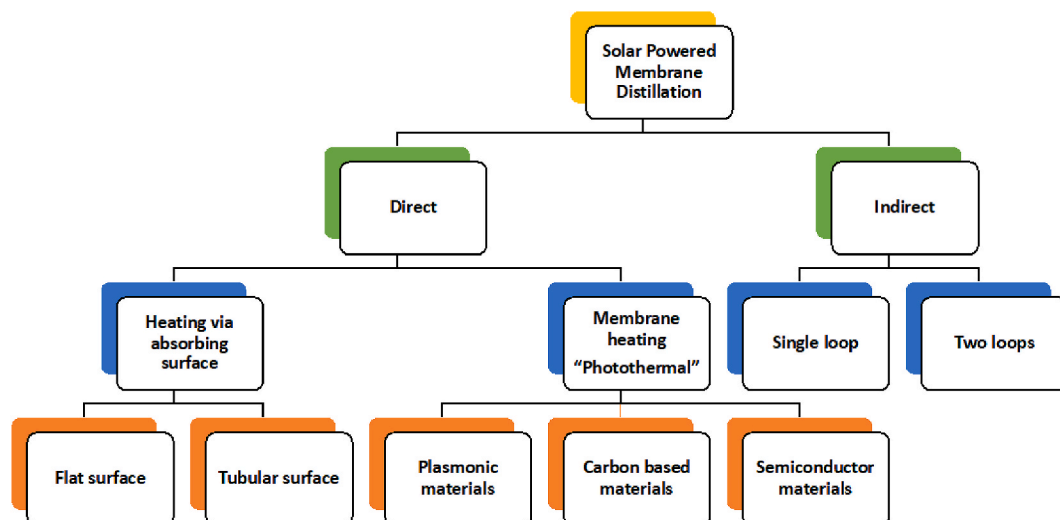


Fig. 3. Classification of MD integrated with solar energy [25].

[22] tested a small AGMD desalination plant powered by solar energy. They used a flat sheet of polytetrafluoroethylene (PTFE) membrane in their research; a feed temperature of 85 °C was set, and a 2.8–8.4 m² total membrane surface area per module was used. A daily permeate flux between 156 and 168 kg m⁻² and a specific heat intake between 810 and 2220 kWh/m³ were required by the system. The authors concluded that a multistage technique is needed to enhance thermal efficiency and the system's effectiveness. Chafidz et al. created fresh water in Saudi Arabia, ranging from 0.27 to 0.38 m³/day, by investigating a compact and hybridized solar-powered vacuum multi-effect MD unit having a 5.12 m² total membrane area [23].

The distillate flux varied around 1.5–2.6 L/m²h, while the typical distillate productivity was 11.53 L/h, reaching a peak of 15.94 L/h at noon, and they concluded that the two tests' solar-energy conversion efficiency was insufficient (33.6 %). Soomro et al. [24] have conducted a comparative and economic study at the pilot scale on various configurations, such as direct contact membrane distillation (DCMD), along with its integration with a solar concentrator. The simulation's results demonstrated that higher irradiance led to greater electricity output. However, the solar power tower (SPT) facility produced the most electricity (353.87 GWh) and had the highest capacity factor (56.1 %). In contrast, the parabolic trough plant had the lowest levelized energy cost (4.51 cents/kWh). Permeate flux increased exponentially for the DCMD system as the feed water temperature rose. The simulation showed that the DCMD system integration with the PT plant allowed for a maximum freshwater production rate of 38.9 m³/day. The SPT plant, combined with the DCMD system, was found to have the lowest cost of water production (0.314 US\$/m³).

3. SPMD configurations and mechanisms

One of the earliest sources still in use today is solar energy. Solar energy has several advantages compared to other energy sources, including cleanliness, sustainability, accessibility in many regions, and a high safety level. Therefore, researchers are working to find methods compatible with solar energy to transform this potential energy source into a suitable form for direct consumption. Technologies based on solar energy can produce drinking water by combining simple methods with cost-effective ideas. Therefore, solar-based technology might be effective in limited populated places where access to drinking water is still a problem. Both direct incorporation and indirect usage are possible with solar-powered desalination systems, and they are categorized as shown in Fig. 3.

Direct desalination systems refer to those employing heat-gathering techniques where desalination and heating processes take place in the same location. In these systems, saline water is subjected to solar radiation, leading to its evaporation. The freshwater is then produced by condensing the evaporated water, illustrating an integrated approach to harnessing heat for desalination. Passive solar stills represent the most straightforward and widely utilized method for direct solar desalination. These stills harness heat through convection and radiation, causing the evaporation of the saline water present beneath the glass cover. The evaporation and condensation processes occur simultaneously during operation. A typical passive solar still can yield up to 5 L per square meter per day [26]. Various types of solar stills exist, including single-slope solar stills (SSSS), double-slope solar stills (DSSS), and Wick-type solar stills. However, the relatively low system efficiency is attributed to the loss of latent heat from condensation on the cover [27].

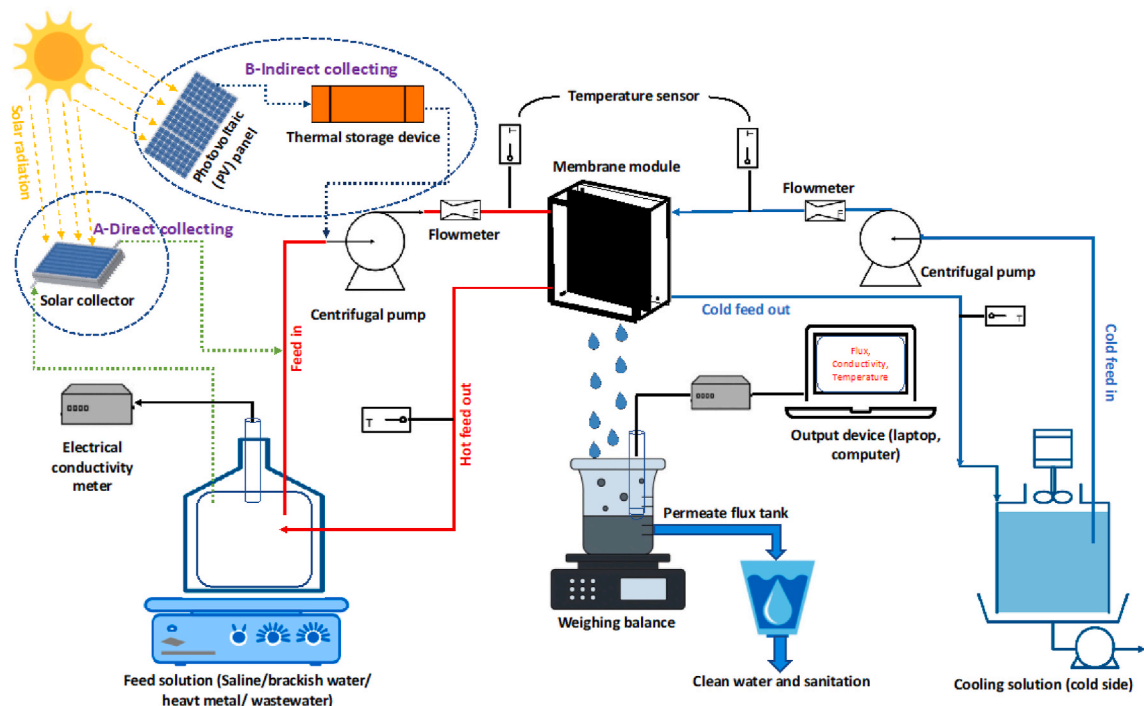


Fig. 4. Configurations for the SPMD system with (A) direct and (B) indirect collecting methods.

To enhance the performance of solar stills, active solar stills have been proposed, incorporating additional equipment such as solar concentrators, condensers, reflectors, solar flat plate collectors, and mechanical agitators. Additionally, researchers have explored multi-effect basin solar stills, where the latent heat is recycled to heat the water in the upper basin, thereby improving overall performance and production efficiency. Multi-basin solar stills have demonstrated high efficiency and effectiveness [28,29]. Extensive research and development efforts have been devoted to refining the design of solar stills and their cover plates [30]. Furthermore, researchers are investigating materials capable of storing latent and sensible heat, such as phase change materials (PCMs), enabling direct solar desalination systems to operate even during non-sunny hours [31]. Moreover, the method for direct heating can be generally categorized into two approaches.

- (a) **Heating via an absorbing surface:** In this process, a top black surface absorbs solar radiation and subsequently transfers the heat to the feed water. This absorbing surface can be either flat, utilizing a flat-sheet membrane, or tubular, employing hollow fiber or capillary membranes.

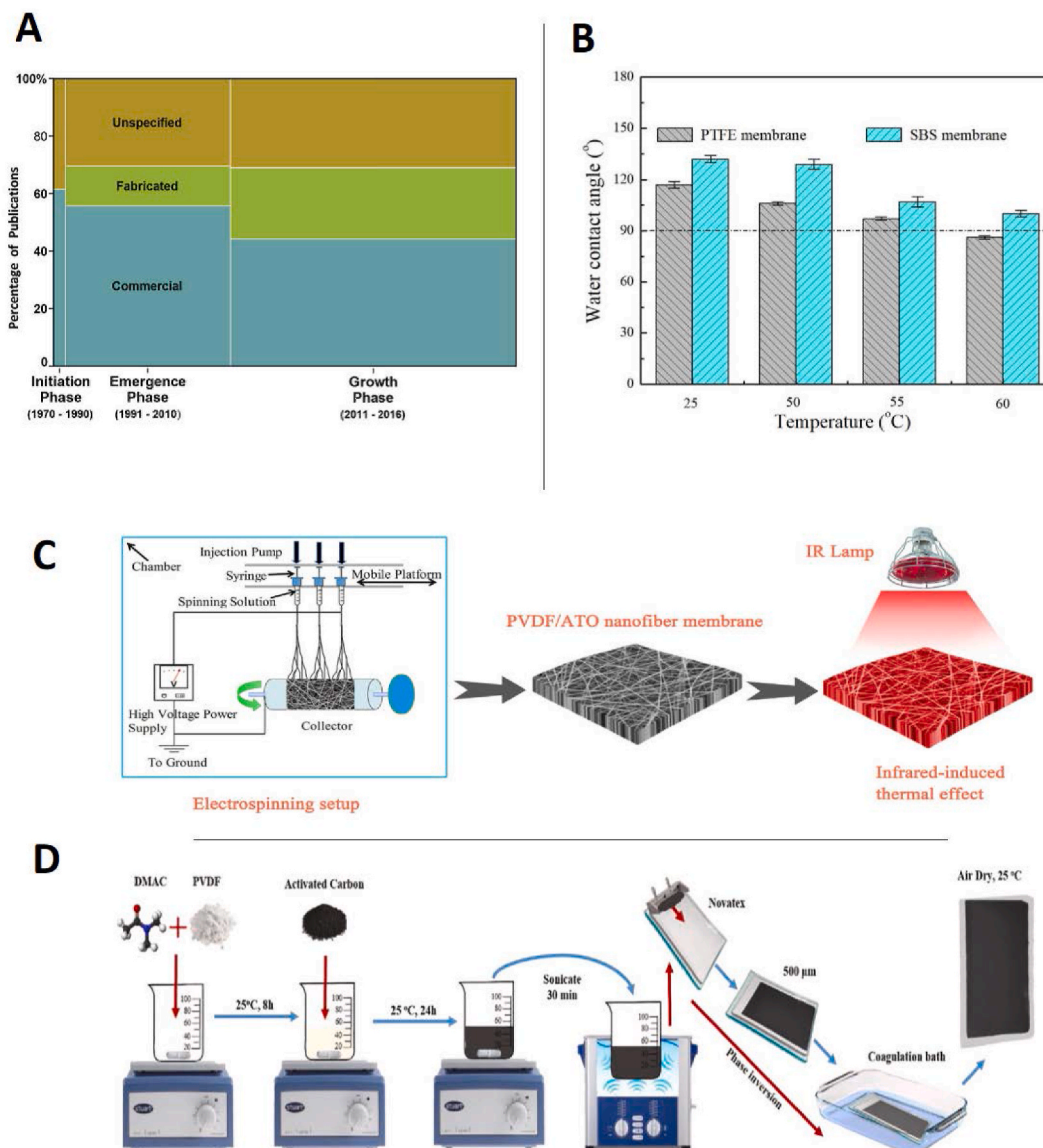


Fig. 5. (A) The percentage distribution of various membrane sources published during the different phases of MD development. Adopted from Ref. [80]. Copyright 2017, Elsevier. (B) Commercial PTFE and fabricated SBS membranes water CA, at various temperatures. The reference liquid was DI water. Adopted from Ref. [81], Copyright 2018, Elsevier. (C) PVDF/ATO photothermal membrane fabrication process using electrospinning technique schematic diagram. Adopted from Ref. [82], Copyright 2019, Elsevier. (D) PVDF/AC membrane fabrication method using phase inversion schematic illustration. It was adopted from Ref. [83] Copyright, 2022, Elsevier.

Table 1
Summary of CMD studies in the literature.

Mem. fabri. approach	Feed Sol.	Mem. area (m ²)	Fabr. method	Coating method	Flux (L/m ² h)	MD config.	Salt rej. (%)	Mem. properties	Mem. material	T _f /T _p (°C)	Ref.
Multi-step	0.5 M NaCl	–	Phase inversion	Laminating machine	3	DCMD	>99.9	D _{avg} : 0.22 μm	PVDF-f-G	70/50	[87]
	3500 mg/L NaCl	0.00145	Commercial	cast drop wise	94	DCMD	–	Θ: 91°, ε: 70 %, D _{avg} : 0.2 μm	PTFE/PVDF-GO	80/20	[88]
	15,000 ppm of a NaCl	0.00145	Commercial	Bilayered	126	DCMD	–	Θ: 125°, ε: 74 %, D _{avg} : 0.45 μm	PTFE/CNT	-/80	[89]
	35 g/L NaCl	0.00747	Commercial	Electrospinning	16.7	DCMD	100	Θ: 132°, ε: 55 %, D _{avg} : 0.25 μm	PTFE/PAN-OH	53/20	[90]
	35 g/L NaCl	–	Commercial	Vacuum filtration	12	DCMD	99	Θ: 113°, ε: 90 %, D _{avg} : 0.22 μm	PES/CNT	65/5	[91]
One-step	35,000 ppm NaCl	0.0026	Commercial	Solution casting	45.1	DCMD	99.9	Θ: 81°, D _{avg} : 0.47 μm	PSf/MWCNT	50/10	[92]
	35 g/L NaCl	0.0032	Commercial	Surface coating	4	VMD	99	Θ: 20°, D _{avg} : 0.2 μm	Fe-CNTs/PTFE	20/-	[93]
	10,000 ppm salt conc.	0.002	Electrospinning		22.2	DCMD	>99.10	Θ: 144°	PcH-PES-PcH/CNTs	65/-	[94]
	35 g/L NaCl	0.002	Electrospinning		29.5	DCMD	99.99	Θ: 159°, ε: 84 %, D _{avg} : 0.29 μm	PcH/CNT	60/20	[95]
	3.5 wt% NaCl	0.00785	Electrospinning		18.5	VMD	99.99	Θ: 152°, ε: 69 %, D _{avg} : 0.49 μm	PVDF-PTFE	-/60	[96]
	3.5 wt% NaCl	0.0021	Electrospinning		22.9	AGMD	99.99	Θ: 163°, ε: 89 %, D _{avg} : 0.86 μm	PVDF/G	60/20	[97]
	3.5 wt% NaCl	–	Phase inversion		45.8	VMD	–	Θ: 127°, D _{avg} : 0.12 μm	PVDF/Ultem®/Al ₂ O ₃	70/-	[98]
	3.5 wt% NaCl	–	Phase inversion		16.7	VMD	99.99	Θ: 144°, ε: 76 %, D _{avg} : 0.41 μm	ECTFE	80/-	[99]
	3.5 wt% NaCl	0.025	Phase inversion		18	DCMD	>99.9	Θ: 101°, ε: 88 %, D _{avg} : 0.4 μm	PVDF/AlFu MOF	60/20	[100]
	35 g/L NaCl	0.00385	Electrospinning		2.87	DCMD	99.99	Θ: 138°, ε: 64 %, D _{avg} : 0.3 μm	PVDF/Fe	48/16	[101]
	10,000 ppm NaCl	0.0019	Phase inversion		41.58	VEDCMD	99.99	Θ: 82°	PTFE/AlFu/PVA	60/20	[102]
	3.5 wt% NaCl	0.0032	Phase inversion		7.2	AGMD	>99.5	Θ: 83°, D _{avg} : 0.47 μm	PVDF/ZIF-8/chitosan	60/20	[103]
	35 g/L NaCl	0.00113	Phase inversion		5.2	VMD	>99.97	Θ: 89°, ε: 71 %, D _{avg} : 0.86 μm	PVDF/MWCNTs/SiO ₂	30/-	[104]
	7.0 wt% NaCl	0.000098	Electrospinning		40	DCMD	99.99	Θ: 154°, ε: 90 %, D _{avg} : 0.76 μm	F-TiO ₂ /PVDF-HFP	60/20	[105]

Abbreviations: Mem.: membrane; Fabr.: fabrication; Sol.: solution; Rej.: rejection; PcH: poly (vinylidene fluoride-co-hexafluoro propylene); f: functionalized; PAN: polyacrylonitrile; ECTFE: ethylene chlorotrifluoroethylene; AlFu: aluminium fumarate; Θ: contact angle; ε: porosity; D_{avg}: mean pore size.

The recent focus of research on direct SPMD systems employing the absorbing surface mechanism has predominantly centred on the utilization of flat-sheet membranes. These modules share a conceptual similarity with flat-plate solar collectors commonly used in domestic hot water systems. Encased beneath the glazed glass, the module incorporates a dark-coloured absorber plate, which absorbs solar radiation, subsequently transferring the heat to the feed water. The heated feed water then flows between the absorber plate and the hydrophobic flat sheet membrane. The resulting vapor traverses through the membrane to the permeate side located at the bottom of the module [32–34].

Chen and Ho employed solar energy as a secondary heat source to heat preheated feed water within a flat sheet DCMD system using a solar simulator. Their study revealed a potential improvement of up to 16 % in solar-assisted MD system efficiency compared to systems lacking direct heating effects. However, it was noted that an increase in flow rate or feed temperature could diminish the enhancement rate, and the system still incurred relatively high water costs compared to conventional desalination systems [35]. Summers and Lienhard evaluated a bench-scale flat sheet AGMD system using a solar simulator to assess the impact of direct solar heating. Vapor is transferred to the air gap on the permeate side, condensing on a cooling copper plate. The module achieved a maximum permeate flux of $0.3 \text{ kg m}^{-2} \text{ h}^{-1}$ and a GOR value of 0.3, with lower flux values attributed to high mass transfer resistance due to the air gap. Furthermore, low feed flow rates were required to absorb sufficient radiation, exacerbating the effects of temperature polarization [32].

A selected number of studies have exclusively focused on numerical simulations of direct SPMD systems employing absorbing plates. Ma et al. developed a numerical model of small-scale, flat-sheet VMD directly utilizing solar energy. They concluded that continuous operation was more efficient in terms of daily water output and energy usage compared to temperature-controlled operation at higher temperatures. With a membrane/collector area of 0.35 m^2 and 12 h of operation, a daily water output of 2.8 kg ($\sim 8 \text{ L/m}^2/\text{d}$) and a GOR of 0.71 were anticipated. The authors later investigated the addition of a heat pump as a heat recovery mechanism, which yielded daily water production of 20.5 L/m^2 and 32 L/m^2 using 0.18 m^2 and 3 m^2 , respectively [36].

Recent endeavors in employing absorbing surfaces in direct solar MD systems have concentrated on constructing structures incorporating multiple effects to harness the energy of condensation. In this approach, only the first effect is directly heated by the absorbing surface. As the vapor passes through the membrane to the permeate side, the latent heat of condensation is utilized to heat the feed in the bottom stages, akin to the multi-basin solar still or multi-stage AGMD designs. Several studies have adopted this concept by employing solar photovoltaic (PV) cells as the heat-absorbing surface, thereby utilizing waste heat that would otherwise be dissipated in conventional PV modules to heat the feed in the first stage. This simultaneous cooling effect enhances efficiency and electrical output. Although promising results have been obtained, scaling up such systems remains challenging due to increased resistance to mass and heat transfer with larger membrane sizes [37].

Wang et al. proposed a photovoltaic-MD (PV-MD) device capable of simultaneously producing electricity and water. This device features multi-stage MD channels integrated on the backside of a solar cell exposed to solar radiation. Waste heat from the solar cell is utilized to heat feed water in the first stage. A 3-stage device achieved a permeate flux of $1.79 \text{ kg m}^{-2} \text{ h}^{-1}$ and an electrical efficiency of 11 % under one sunlight [38]. Similarly, Antonetto and colleagues investigated the performance of an integrated system combining membrane distillation (MD) membranes and photovoltaic (PV) technology. In their setup, the desalination system was positioned behind the PV panels. Utilizing the low-temperature heat recovered from the backside of the PV system, the passive distillation desalination system operated without the need for additional electrical or mechanical components. The study aimed to assess the feasibility of simultaneously generating electricity from the PV system and producing fresh, potable water using waste heat. Experimental and numerical analyses were conducted to evaluate the system's performance. Results indicated that under 1 sun irradiance, the device could produce potable water at a rate of $2 \text{ kg m}^{-2} \text{ h}^{-1}$ with an energy requirement of approximately 670 kWh/m^3 . Additionally, integrating the desalination system led to a 4.5 % increase in PV efficiency, attributed to a reduction in the PV device's temperature by about 9°C [39].

b) **Membrane's surface heating:** In this process, solar radiation is absorbed by a photothermal material, converting light energy into heat energy. This photothermal material can be layered or coated onto a membrane, effectively heating the membrane surface. In essence, the feed water is heated directly at the membrane surface (as illustrated in Fig. 1B) rather than being heated from an upper absorbing surface (as depicted in Fig. 1A). As some researchers have noted, a significant challenge with the absorbing surface mechanism in direct SPMD systems is the need for a considerable reduction in feed flow rate to effectively absorb solar radiation. This low flow rate exacerbates temperature polarization, adversely affecting permeate flux. To address this issue, scholars have proposed heating the membrane itself to counteract temperature polarization and enhance MD performance. This approach involves three techniques: joule heating, induction heating, and solar photothermal membranes [40].

The concept of directly heating the membrane was first introduced by Summers and Lienhard [41], who utilized a two-layer membrane with a black hydrophilic layer atop a hydrophobic PVDF membrane in an Air Gap Membrane Distillation (AGMD) configuration. They found that heating the membrane surfaces instead of using an absorbing surface was more effective in terms of permeated flux and efficiency due to reduced heat loss to the environment and decreased heat transfer resistance. Other researchers have explored novel membrane designs to enhance heating efficiency. Politano et al. developed a nano-enhanced membrane by incorporating silver nanoparticles (AgNPs) into a PVDF membrane, which exhibited improved performance in efficiency and permeate flux compared to a virgin membrane [42]. Similarly, Wu et al. coated a PVDF membrane with polydopamine (PDA) to achieve localized heating in a DCMD configuration, demonstrating significantly higher permeate flux under solar irradiation [43]. Recent studies have focused on innovative materials and fabrication methods to enhance photothermal membrane performance. Researchers have experimented with various nanoparticles, including carbon black, Fe_3O_4 , and titanium nitride, to improve light-to-heat

Table 2
Summary of PMD studies in the literature.

Mem. fabri. approach	Feed Sol.	Mem. area (m ²)	Fabr. method	Coating method	Flux (kg/m ² h)	MD config.	Irradiation (kW/m ²)	Salt rej. (%)	η (%)	Mem. Properties	Mem. material	Ref.
Multi-step	Organic pollutants and salts	0.000081	–	Electrospinner/PVA	1.31	–	1	>99.8	78	T _m : 330 K	PVDF/Carbonized eggshell - CNT	[108]
	200 mg/L BSA in 10 g/L NaCl	0.0037	–	dip coating	0.89	DCMD	5.5	–	–	–	MXene-coated PVDF	[109]
	16.70 wt% NaCl	0.0004	–	scalable spraying	0.78	DCMD	1	99.6	66.8	D _{avg} : 0.45 μm; T _m : 314 K	PVDF/FTCS-CB	[110]
	0.5 M NaCl	0.0009	–	scalable spray-coating method	1.17	AGMD	0.75	–	105	T _m : 325 K	FTCS-PDA/graphene/PTFE	[111]
	3.5 % NaCl	0.0012	Electrospinning	Spray coating	1.01	DCMD	1	99.9	66.7	ε: 70 %; D _{avg} : 0.2 μm; T _m : 324 K	TiN/PVDF	[112]
	brackish groundwater	0.002	–	Spray-coating	0.76	DCMD	2.8	–	–	D _{avg} : 0.2 μm	CB-PVDF	[77]
	35 g/L NaCl	0.0031	–	drop coating & capillary coating	3.19	DCMD	1	99.9	75.4	D _{avg} : 0.2 μm; T _m : 321 K	CB-PVDF	[5]
	3.5 wt% NaCl	0.0016	Electrospinning	Spraying	1.43	–	1	99.9	60	T _m : 344 K	PDMS/CNT/PVDF	[113]
	35 g/L NaCl	0.0019	Commercial	electro-spun/PVA	0.94	AGMD	1	>99.9	64.1	D _{avg} : 0.2 μm; T _m : 332 K	TiN@PVA-PVDF	[114]
	3.5 wt% NaCl	0.00018	Electrospinning	Vacuum filtration	0.97	DCMD	1	99.99	53	T _m : 323 K	Fe ₃ O ₄ /PVDF-HFP	[115]
–	–	–	Vacuum filtration	0.89	DCMD	1	–	62	T _m : 320 K	HA@PDA/HA-CS film	[116]	
3.5 wt% NaCl	0.0007	Electrospinning	Vacuum filtration /PDMS	1.3	DCMD	1	>99.9	81.6	ε: 80 %; T _m : 370 K	PPy NTs/PVDF	[117]	
One-step	3.5 wt% NaCl	0.00196	Electrospinning		27	VMD	0.1	>98	–	ε: 77 %; T _m : 367 K	PVDF/ATO	[82]
	0.5 M NaCl	–	Bilayered aerogel		9.4	DCMD	9	>99.9	72	ε: 93 %; T _m : 529 K	FTCS-PDA/BNC	[118]

Abbreviations T_m: maximum membrane surface temperature reached; BNC: bacterial nanocellulose; TiN: titanium nitride; PPy NTs: polypyrrole nanotube.

conversion efficiency. Additionally, bio-derived materials such as carbonized eggshell membrane and polydopamine have been investigated for their potential in photothermal membranes [44,45]. Novel membrane structures, such as Janus membranes and hybrid nanofiber composites, have been developed to further enhance heating efficiency and anti-fouling properties. These membranes have demonstrated promising results in terms of permeate flux and stability under solar irradiation [46]. Overall, ongoing research in photothermal membranes for direct SPMD systems aims to address challenges related to TP and low permeate flux while maximizing energy efficiency and sustainability. These efforts involve a combination of material innovation, membrane design optimization, and advanced fabrication techniques to realize the full potential of solar desalination technology. More details about this approach to direct heating are discussed in the next section, which is the focus of this paper.

In the indirect approach to desalination, an extra step is incorporated to utilize solar energy, which can function as either a heat source or a power-generating element. These systems, known as solar collectors, effectively leverage solar thermal energy to improve the desalination process. Essentially, they enhance desalination by efficiently utilizing the potential of solar heat [47]. Solar collectors come in a variety of designs and uses. Compared to flat-plate kinds, evacuated tube collectors work more efficiently at high temperatures [48,49]. Evacuated tube collectors are more effective on foggy days than cylindrical tracking collectors. The energy source that generates temperatures of 120 °C or higher should be tracked precisely by the detailed mechanisms that parabolic concentrating collectors possess.

Three layers of salty water with different salinity profiles make up a solar pond, which is another solar thermal collector device for water desalination. While the water at the top has a low concentration, the concentration near the bottom is higher. Sunlight will be trapped by the dense concentration at the bottom [50]. While the surface water is cold, the high salinity water is heated by the absorbed light until it boils. The temperature in this bottom layer, known as the solar pond, reaches almost 100 °C [51]. Utilizing this hot brine water and a specialized organic-fluid turbine, electricity can be produced. In addition to producing electricity, solar ponds can store energy. The highly concentrated stream (brine) that desalination plants discard is an excellent prospective supply for usage in solar ponds that should be highlighted. Considering this, solar ponds are an appropriate side system, or cooperator, for desalination plants [48–50].

Another silicon-cell-based technology that is readily available is photovoltaic (PV) panels or modules. Solar radiation is absorbed by the cells, which then turn it into electricity (direct current, or DC). There are several benefits to using PV panels, including their long lifespan, lack of moving parts, ease of maintenance, ability to alter power production in parallel or series, and lack of sound or environmental pollution [52]. PV modules, however, may only be a desirable option in nations where the cost of the commonly given energy is high because the final prices are still not competitive with those of other energy sources [53,54].

According to Al-Obaidani et al. [55], a membrane-based desalination technique called MD is compatible with solar power installations. Furthermore, due to MD's tolerance for varying and intermittent working conditions, as well as its need for low-grade thermal energy,

combining the MD system with solar energy has been an intriguing prospect around the world. Fig. 4 shows two different solar energy coupling arrangements for the MD systems. Solar thermal collectors are part of the solar-assisted MD desalination unit and supply hot water to the MD module. It should be emphasized that all pumps and other equipment are powered by either the electrical grid or the generator, and that heat is given to the MD module either directly or through a heat exchanger.

Fig. 4A commonly depicts this setup. Specifically, SPMD is a hybrid system in which off-grid electricity is used. According to this definition, a hybrid system generates energy off the grid and provides heat and power to its end users. The essential components of the solar standalone DCMD configuration are the solar thermal collector/photovoltaic module, the feed and distillate tank, the MD module, and the circulation pumps. The standalone solar MD desalination configuration, which is depicted in Fig. 4B—is identical to the solar-assisted configuration in all respects, except that the required electricity is provided by solar-powered PV collectors integrated with DC batteries and electrical current inventors rather than a diesel generator.

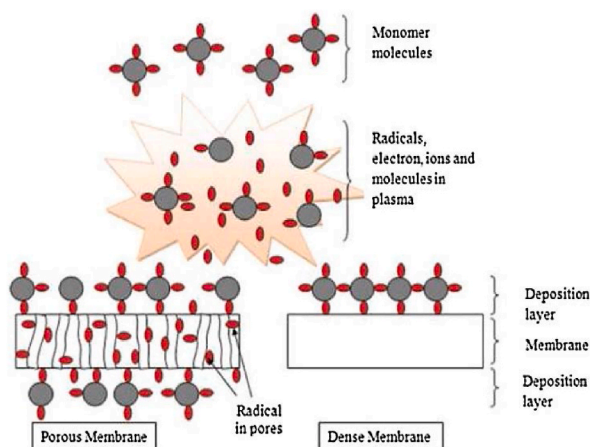


Fig. 6. Plasma polymerization mechanism for the deposition of a thin film. Adopted from Ref. [121]. Copyright, 2020, MDPI.

4. Conventional and solar-powered membrane distillation membranes' characteristics

4.1. Membrane characteristics criteria

In the MD process, non-wetting membranes are often used. The primary features of these microscopic membranes are their hydrophobic qualities. Many polymers, including PTFE [56], polypropylene (PP) [57], and polyvinylidene fluoride (PVDF) [58], have been employed to make these membranes. To assess the membrane's susceptibility to wetting, the liquid entry pressure (LEP) parameter must be evaluated. According to the literature, values between 0.5 and 4.6 bar have been used [59,60]; however, the LEP of the feed solution should be greater than 2.5 bar for the MD plant to operate properly [61]. The Laplace equation is used to describe LEP:

$$LEP_w = \frac{B \gamma_L \cos \theta}{r_{max}} \quad (2)$$

where B represents the pore structure geometric factor (equal to 1 for cylindrical pores), θ is the liquid/membrane contact angle (CA), γ_L is the liquid surface tension, and r_{max} is the maximum pore size [62]. Therefore, the membrane material should have low interface energy between the liquid and the membrane, high surface tension, and a small pore size to achieve high LEP.

Furthermore, porosity and pore size are crucial properties of MD membranes. Generally, a high porosity membrane can produce greater permeate flow, a larger evaporation surface area, and reduced conductive heat loss. The most common method for determining membrane porosity is to use isopropyl alcohol (IPA). The Smolder-Franken equation [63] can be used to calculate porosity (ϵ):

$$\epsilon = 1 - \frac{\rho_m}{\rho_p} \quad (3)$$

where ρ_p and ρ_m are the densities of the polymer material and the membrane, respectively. Since the mechanical strength of the membrane limits porosity, it is considered the most important characteristic [64]. The porosity values reported in the literature range from 40 % to 90 %; however, a porosity value of around 80 % is recommended [65]. When it comes to pore size, any size lying between 0.1 and 1 μm is considered suitable, as it avoids membrane wetting [66,67]. Experimentally, increasing the pore size of the membrane causes an enhancement in permeate flux. The impact of pore size distribution on MD flux has been extensively researched. Researchers have found that the mean pore size affects the vapor transfer coefficient mainly, not the pore size distribution [68–70].

The thickness of the membrane is another significant factor in achieving optimal performance. Vapor flow across the membrane is strongly affected by its thickness. A thicker membrane increases mass transfer resistance, thereby lowering vapor flow and heat loss. Several studies show that the appropriate membrane thickness for an MD membrane should be in the 100–700 μm range. However, it should be noted that this range might vary based on membrane characteristics, process conditions, and feed concentration. For example, different studies evaluating the impact of membrane thickness at various salinities for DCMD configurations suggested that membrane thicknesses of $\approx 739 \mu\text{m}$ and $\approx 13 \mu\text{m}$ are optimum for NaCl concentrations of 24 wt% and less than 10 wt% [71,72].

A temperature difference is the driving force of the process; therefore, the conductivity of the membrane material is a crucial consideration during membrane design. Less heat loss throughout the process results in increased energy efficiency and less sensitivity to temperature polarization events, allowing for enhanced flux across the membrane. Polymers have thermal conductivities ranging

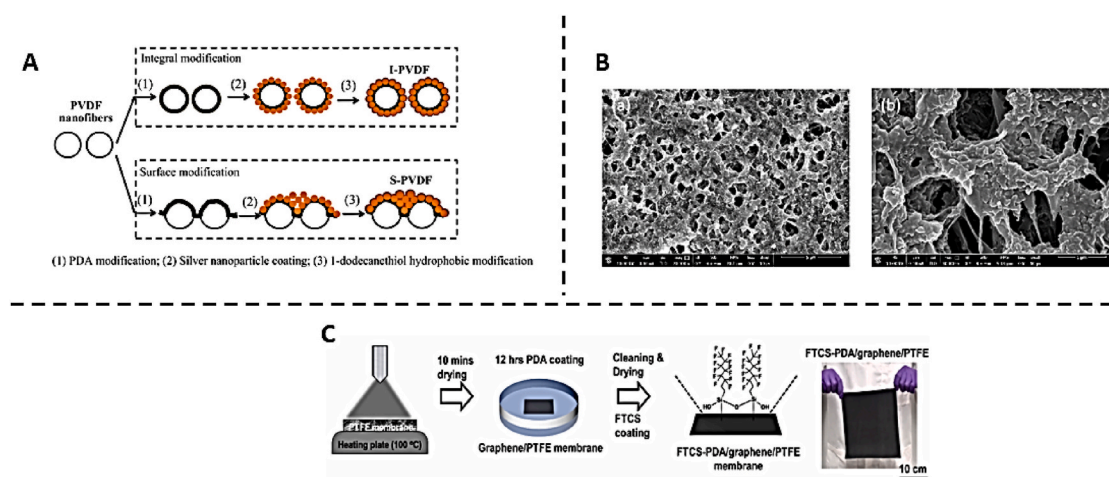


Fig. 7. (A) Schematic diagram of the preparation of modified PVDF nanofiber membranes by PDA, Ag NPs, and 1-dodecanethiol hydrophobic. Adopted from Ref. [127]. Copyright, 2013, Elsevier. (B) 0.2 wt% FAS17/CB coated membrane SEM surface images at (a) low-resolution (5 μm) and (b) high-resolution (2 μm) at operating conditions of 150 mL/min permeate and feed flowrates, $T_p = 20 \text{ }^\circ\text{C}$, and $T_f = 35 \text{ }^\circ\text{C}$, and 1 sun irradiance. Adopted from Ref. [5]. Copyright, 2021, Elsevier. (C) Schematic diagram of the fabrication of FTCS-PDA/graphene/PTFE membrane and a photographic image of the final prepared membrane. Adopted from Ref. [111]. Copyright, 2021, Elsevier.

from 0.1 to 0.5 W/mK. It is determined by the temperature, degree of crystallinity, and crystal shape [73]. Various approaches have been proposed to reduce heat loss by membrane conduction [74]. The use of membrane materials with poor thermal conductivities, a thicker membrane, and a highly porous membrane is among these techniques.

In addition to the membrane criteria for MD systems mentioned above, the membranes must have anti-scaling and anti-fouling properties. Furthermore, for long-term operation, the thermal and chemical stabilities of the membrane material are crucial, particularly in the SPMD process [75–77], as solar radiation can decompose or degrade membrane materials, significantly reducing their performance and stability. Lastly, it is recommended that the CA be $> 90^\circ$ to ensure a membrane layer with hydrophobic properties [78,79].

4.2. Membrane fabrication through a one-step approach

Only commercial membranes were used when MD was founded in the late 1960s (initiation phase). The use of commercial membranes remains predominant in the publications of the 2000s (emergence phase) and current (growth phase) publications, at 56 % and 44 %, respectively [80]. However, there is a growing trend in fabricating 'MD specific' membranes in-house and fine-tuning membranes by grafting, blending, surface modification, and other methods. As seen in Fig. 5A, the fraction of laboratory-fabricated membranes increased from 14 % to 25 % during the growth period. This reflects an increase in expertise in membrane fabrication among diverse MD research groups around the world, as well as an increase in interest in the invention of novel membrane materials. This section will discuss the one-step membrane fabrication methods used, which are done by preparing dope solutions.

Two of the most common one-step fabrication methods widely used across the literature for both CMD and SPMD systems are electrospinning and non-solvent induced phase separation (NIPS), which result in the formation of mixed matrix membranes (MMMs). MMMs are those that combine a solid phase (e.g., nanomaterial) within a matrix material (e.g., polymer). One of the benefits of using either fabrication method is the utilization of the different polymers that can be used for MD membrane fabrication, as opposed to commercial MD membrane synthesis, which is limited to polymers such as PTFE, PP, and PVDF. For example, styrene-butadiene-styrene (SBS) has recently been electrospun into a nanofibrous MD membrane, and the results demonstrated that the SBS electrospun membrane was more hydrophobic than the commercial PTFE membrane (Fig. 5B) [81]. In addition, it opened doors for exploring new hydrophobic polymers for MD and coming up with novel hydrophobic polymer blends. For instance, the solubility of various fluorinated copolymers in the solvents utilized is significant in increasing the hydrophobicity and tensile strength. Therefore, such copolymers can be used to create microporous hydrophobic membranes for desalination purposes. As a result, research has been conducted to improve performance by mixing highly hydrophobic PTFE with soluble PVDF [84]. Another study by Zuo et al. [85] developed a dual-layer PVDF/Ultem1 membrane for a VMD desalination setup. Hyflon1 AD, another attractive fluoropolymer, was recently developed [86]. Table 1 includes the MD performance of various new polymers. Yet, more research on membrane manufacturing processes for these unique polymers is required to improve the performance of the specialized membrane for MD.

Generally, the electrospinning method is used more frequently than NIPS when it comes to fabricating SPMD membranes. As a result, while the use of electrospinning for membrane applications is becoming more common in the literature, it is still quite costly to scale up compared to traditional approaches such as NIPS. Currently, its key applications are in biological applications where the cost-benefit ratio has been demonstrated. However, certain advances (e.g., the Stellenbosch Nanofiber Company developed the usage of a revolving perforated ball in place of several syringe heads) [106] are resolving these issues, and as a result, the demand for nanofiber membranes is expected to increase in the future.

The fundamental benefit of one-step production technologies (NIPS and electrospinning) is that photothermal materials may be

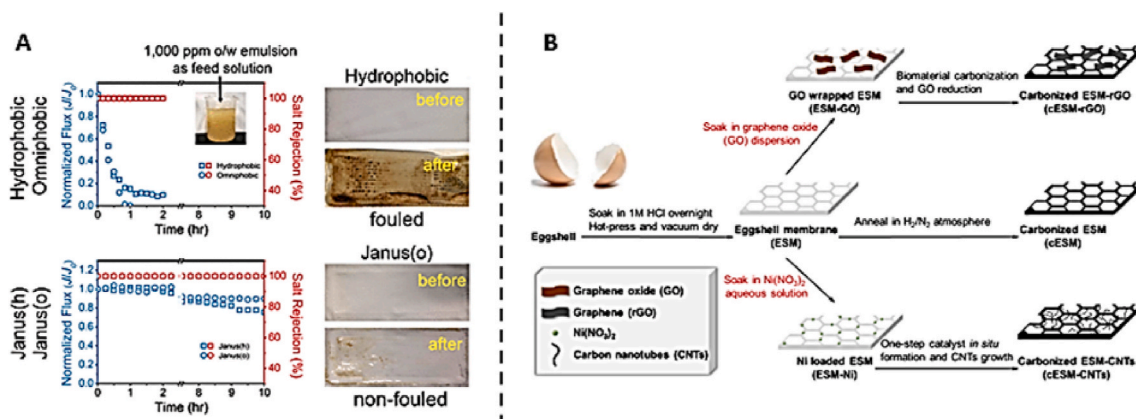


Fig. 8. (A) Normalized water fluxes (blue) and salt rejections (red) for MD fouling experiments with Janus and hydrophobic membranes. Photographic images of hydrophobic and Janus membranes before and after fouling experiments (operating conditions: $T_p = 20^\circ\text{C}$, $T_f = 60^\circ\text{C}$, feed solution: saline oil-in-water emulsion with 1000 ppm crude oil and 35 g/L NaCl). Adopted from Ref. [129]. Copyright, 2017, American Chemical Society. (B) Schematic diagram for preparation of bio-derived ultrathin hierarchical porous membranes. Adopted from Ref. [108]. Copyright, 2019, Elsevier.

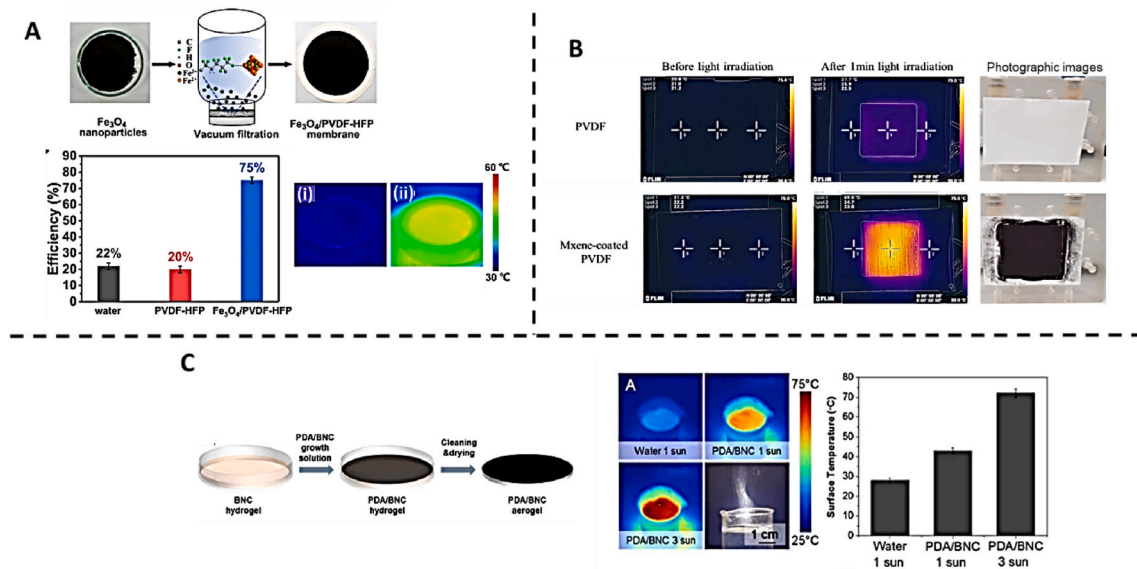


Fig. 9. (A) Fe₃O₄/PVDF-HFP membrane fabrication process. The photothermal efficiency under 1 kW/m² solar irradiation. IR camera images of the pristine (i) and Fe₃O₄/PVDF-HFP (ii) membranes under the illumination of 1 kW/m² after 20 min of illumination. Adopted from Ref. [115]. Copyright, 2020, Elsevier. (B) Pristine PVDF and MXene-coated PVDF membranes: IR thermal images before and after 1 min of light irradiation and photographs of the feed surfaces after 21 h of filtering a 10 g/L NaCl and 200 mg/L BSA feed water. Adopted from Ref. [109]. Copyright, 2018, Elsevier. (C) Bi-layered PDA/BNC film fabrication process schematic illustration. IR images of water and PDA/BNC film under 1 and 3 kW/m² irradiation and a digital photograph demonstrating steam generation. Adopted from Ref. [131]. Copyright, 2017, Royal Society of Chemistry.

distributed and uniformly incorporated into polymeric membrane substrates. As a result, there is no possibility that photothermal particles will leak into permeable water. Meanwhile, as compared to two-step fabrication techniques, these methods are simple to scale up. However, it requires a large volume of extremely expensive photothermal materials, which do not all necessarily add to the efficiency of light-to-heat conversion as they are hidden beneath the membrane surface. Fig. 5C and D demonstrate the membrane fabrication methods via electrospinning and NIPS techniques, respectively.

4.3. Membrane fabrication approach: multi-steps

An extensive study has been devoted to improving the performance of membranes in MD applications using a variety of approaches. The major attribute that contributes to the increase in MD performance is hydrophobicity. Hydrophobicity is fundamentally

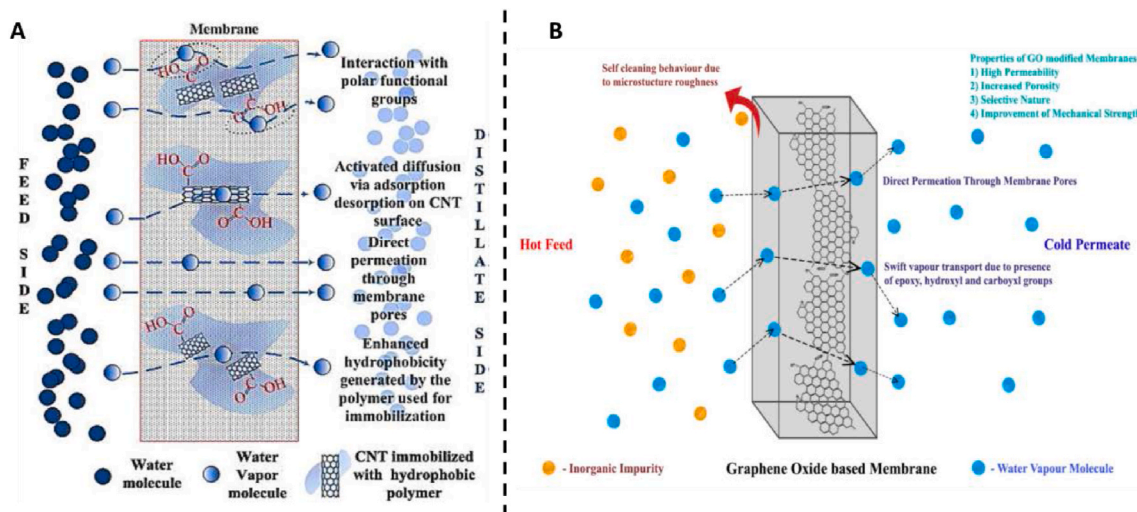


Fig. 10. (A) CNT mechanism in MD membranes. Adopted from Ref. [140]. Copyright, 2014, Elsevier. (B) Performance enhancement in MD membranes due to the addition of GO NPs.

determined by factors such as membrane microstructure, surface chemistry, and surface roughness [107]. To attain better performance, multi-step surface modifications have been used to increase the hydrophobicity and properties of the desired membrane in MD. The membrane surface modifications are performed by depositing a thin functional layer onto the membrane's outer surface, and this is the simplest method for increasing the membrane's surface hydrophobicity. Although surface modification approaches such as the use of polydopamine (PDA), dip coating, and vacuum filtration are excellent for coating functional substances on membrane surfaces, the homogeneity, thickness, and long-term use of the coated layer require further investigation, especially under harsh conditions. During the cleaning or operation procedures, the coated layer can be wiped away. As a result, chemical changes, e.g., cross-linking or sulfonation, are frequently performed on the surface of deposited coated membranes to improve durability. The most successful surface modifications for both CMD and SPMD will be discussed in the next section. Further, Tables 1 and 2 include various studies in which nanoparticles (NPs) are attached to the membrane using the mentioned approaches.

4.3.1. Plasma treatment

Plasma treatment is an effective chemical modification approach for anchoring functional graft chains and generating active groups on the surface of the membrane. The membrane surface hydrophobicity can be increased because of the rise in fluorine concentration when the surface is grafted with fluorinated monomers. This technique does not change the membrane matrix; however, it can be used as a post-treatment to achieve the necessary properties [119]. Ionized gas polymerization and adsorption on the fibre surface are part of the plasma technique. During plasma polymerization, monomer polymerization under vacuum treatment can form a thin and transparently coated layer. This costly vacuum equipment is a significant disadvantage of the plasma method [120]. Plasma polymerization for thin film deposition is seen in Fig. 6.

Plasma treatment can be used to increase the surface wettability of hydrophilic and hydrophobic membranes [122]. Shen et al. [123] and Yang et al. [124] investigated the chemical and plasma activation of the hydrophobic PVDF membrane surface. Their findings show that the CA of the membranes increases from 80° to 141° and from 105° to 115° , respectively. Similarly, Wei et al. [125] transformed a hydrophilic asymmetric polyethersulfone (PES) membrane into a hydrophobic PES membrane using CF_4 plasma modification. Stable membrane performance was achieved when the membrane surface was modified with a fluorinated layer. The LEP and the CA increased by 370 kPa and 53 %, respectively, due to an increase in the concentration ratio of fluorine to carbon atoms. The modified PES membrane showed a steady flow of $66.7 \text{ kg/m}^2\text{h}$ and a 99.97 % salt rejection at 73.8°C during a 54-h DCMD experiment.

The use of plasma in solar MD is relatively rare in the literature. A study reported using the modified plasma-enhanced chemical vapor deposition (CVD) technique, a vertical graphene was created, which is a novel 3D graphene structure. A micro-interconnected, homogeneous, dense 3D graphene structure, along with a macroporous Ni foam used as a substrate, achieved effective heat and light localization, which improved the efficiency of photothermal conversion. The 3D graphene/Ni foam was then sprayed with a poly(3,4-ethylenedioxythiophene) poly(styrenesulfonate) solution to create P-G-Ni foam, an advanced nanostructured light absorber. The microstructures of the 3D graphene created from the plasma achieved effective water transport to the solar absorber layer/P-G-Ni foam surface, as well as good antifouling properties. Under solar radiation, the water vapor production and photothermal conversion efficiencies were 82.3 % and 73.4 %, respectively [126]. The novel smart system design and plasma-synthesized 3D graphene microstructure overcome the limitations associated with designs and conventional materials for photothermal MD, such as photothermal conversion efficiency, low water vapor flux, heat dissipation, and membrane fouling. This study proves how the uniqueness of the nanomaterials created by a plasma technique may lead to high-performance solar-driven efficient MD technologies and next-generation solar harvesting.

4.3.2. Using polydopamine as a glue

PDA can be readily coated on a variety of substrates by self-polymerization, independent of morphology or surface energy [127]. Furthermore, PDA is an environmentally beneficial choice for water treatment because of its biocompatibility and low toxicity. As a result, PDA has been utilized to fabricate membranes for MD systems. For example, for DCMD, using electrospinning technology, Liao et al. [127] created a very hydrophobic surface on PVDF nanofiber membranes. After chemical reduction, PDA was employed to cover the nanofibrous surfaces, which were then coated with silver nanoparticles to increase the form and roughness of the membrane (Fig. 7A). The CA was extended to 150° due to this surface modification, and a high and consistent MD water flux of $31.6 \text{ L/m}^2\text{h}$ was achieved.

PDA also has a strong photothermal conversion characteristic as well as a broad light absorption spectrum. As a result, several studies have used PDA as an intermediate adhesive or a chemically modified layer in the fabrication of PMD membranes. Carbon black (CB) NPs and 1H, 1H, 2H, 2H-perfluorodecyltriethoxysilane (FAS17) were adhered to the surface of a commercial PVDF membrane using PDA as glue, as reported by Li et al. [5]. The membrane surface was coated with FAS17/CB NPs, which gave the membrane an omniphobic property and increased its CA from 0 to 94° in addition to absorbing light and providing localized heating for PMD. Furthermore, the membrane flux and the utilization efficiency of solar energy in the direct solar membrane distillation (DSMD) process increased by 25 % and 10 times higher, respectively, when compared to the energy efficiency of the conventional DSMD process upon simulated solar irradiation at one solar unit. Moreover, the membrane flux rose by 25 %, and the DSMD process's solar energy usage efficiency was 75.4 %, which is more than one order of magnitude greater than the typical DCMD process. After five DSMD experiments, the utilization of PDA achieved a strong attachment between the PVDF membrane and CB NPs, as the secondary nanostructure on the membrane surface remained intact (Fig. 7B). Furthermore, as shown in Fig. 7C, using PDA and FTCS, GNSs were spray-coated on the surface of the PTFE membrane [111]. After 60 s of 0.75 kW/m^2 light, the resulting membrane can quickly reach 52°C . In the future, PDA will allow for the grafting of more effective photothermal materials onto the surfaces of membrane substrates.

4.3.3. Dip coating

Dip coating entails the application of a thin photothermal material dispersed in a solution layer to the membrane's surface. This straightforward process is divided into five categories: immersion, start-up, deposition, evaporation, and drainage. The concentration of cross-linking agents, dip time, and dipping polymer concentration impact the membrane pore size, membrane structural integrity, and coating material thickness [128]. Huang et al. created a novel Janus membrane for desalinating a hypersaline brine solution stream in an MD process, with amphiphilic wetting and hydrophobic foulant agents to overcome fouling and wetting. A CTAB/polyvinylidene fluoride-hexafluoropropylene (PVDF-HFP) electrospun nanofibrous layer was synthesized, and the nanofibrous substrate was dip-coated with Si NPs before being fluorinated using CVD. The nanoparticle-coated substrate was kept under vacuum at 100 °C for 1 day, while being exposed to 0.15 mL of fluoroalkyl silane, to fluorinate the Si NPs via CVD. After 10 h of operation, visual observation throughout the MD process indicated that the unmodified PVDF/HFP membrane was severely fouled (Fig. 8A) [129].

In addition, Han et al. [108] created eggshell composite membranes for a PMD technique. Mould-graphite-assisted vacuum-drying eggshells were used to produce the eggshell membranes (ESMs), which were then heated to carbonized eggshell membranes (cESM) (Fig. 8B). The ESM was immersed in graphene oxide (GO) dispersion, carbonized, and reduced to create an rGO-wrapped ESM. To make the cESM-Carbon nanotubes (cESM-CNT) membrane, the ESMs were first dipped in a precursor solution and subsequently in a CNTs growth solution. The porous morphologies of the rGO-wrapped and cESM ESM were identical; however, the CNT-functionalized membrane had a fluffy structure coated by CNTs. The cESM-CNTs demonstrated a rapid temperature rise to 330 K due to both CNTs and cESM's improved light absorption capacities providing a foundation for their PMD application.

4.3.4. Vacuum filtration

Various materials can be readily deposited on the membrane surface during the vacuum filtering process. The thickness of the coating layer may be simply adjusted by the concentration and volume of the photothermal material coating solutions, in addition to the ease of operation. CNTs were synthesized into paper-like structures known as Bucky-Papers (BP) as self-supporting membranes in a recent study [130]. The vacuum filtering of CNTs dispersed in 99.8 % pure 2-propanol resulted in ultra-thin BP membranes with narrow pore sizes. At a water vapor partial pressure differential of 22.7 kPa, the self-supporting CNT BP membrane demonstrated a DCMD flow of 12 LMH with 99 % salt rejection. However, debonding and aging have been reported; therefore, modifications such as surface grafting must be implemented to increase membrane durability.

Similarly, vacuum filtration has been used more extensively for the preparation of photothermal membranes. For example, in PMD applications, nanofibrous PVDF membranes were vacuum filtered with iron (II, III) oxide (Fe_3O_4) NPs, as illustrated in Fig. 9A [115]. Due to the excellent photothermal conversion capabilities and light absorption of Fe_3O_4 NPs, under an illumination of 1.0 kW/m², the membrane surface temperature increased by 25 °C in 10 min. In addition to electrospun nanofibrous membranes, commercial membrane substrates have been employed as suitable vacuum-coated photothermal layer substrates. A commercial PVDF micro-filtration (MF) membrane's surface was vacuum filtered using MXene, which is a novel emergent 2D material, as illustrated in Fig. 9B [109]. They were filtered on the PVDF membrane surface to create a photothermal skin layer with localized heating because of their superior photothermal efficiency and optical absorption. After 1 min of 50W LED irradiation, the PVDF membrane coated with MXene had a large temperature rise of 49 °C, as demonstrated by the infrared (IR) thermal image. These photothermal materials disposal might threaten the ecosystem and the environment because they are non-biodegradable and non-biocompatible. As a result, as shown in Fig. 9C—a biodegradable bi-layered photothermal evaporator was proposed for very efficient solar steam production, made of bacterial nanocellulose (BNC) that has been heavily loaded with PDA particles throughout the growth process [131]. Floating at the air/water interface, the PDA/BNC surface temperature increased to 43 °C and 72 °C under 1.0 and 3.0 kW/m² irradiation, respectively. The rapid evaporation of water from the large increase in temperature of PDA/BNC film under 3 kW/m² irradiation was quite evident from the appearance of steam.

Although the vacuum filtering technique offers considerable advantages, such as ease of operation, the scaling up of photothermal membranes for vacuum filtration is challenging because of the vacuum system size restrictions. Moreover, due to the unusual bonding interactions between the membrane substrates and the coating layers, it is also important to investigate the chemical and thermal stabilities of the coating layers.

4.4. Various fillers utilized to modify MD and SPMD membranes

Different fillers have been critical to the progress and development of MD and SPMD membranes. Several studies on the integration of nanomaterials into various MD systems for desalination applications have been done. Moreover, metal-organic frameworks, graphene, CNTs, and metallic NP have been utilized to provide the desired membrane structural and functional features. These materials provide membranes with excellent qualities, including thermal stability, mechanical strength, anti-fouling nature, chemical resistance, and selective permeability, resulting in enhanced functional and operational properties.

Similarly, different studies have shown that nanofluids are being successfully incorporated into PMD membranes. Nanofluids are nanoparticle suspensions that have a high capacity to absorb solar energy and, hence, increase solar absorption efficiency. As a result, they have recently garnered interest as heat transfer fluids [132–135], and researchers are currently examining how nanofluids might improve the efficiency of solar-powered MD systems. Metallic oxides/nitrides, carbon-related nanoparticles, and metals are also popular nanofluid precursors. According to Peng Wang [136], developments in nano-enabled photothermal materials fuelled the rebirth of solar-powered desalination. SPMD has been the subject of numerous recent and ongoing investigations involving photothermal nanoparticles, intending to decrease thermal energy needs, which may account for up to 70 % of the total MD system cost [80]. Therefore, the effects and use of the commonly used nanomaterials on membrane modifications in MD and SPMD seawater

desalination applications are discussed in detail in this section. Tables 1 and 2 also show a brief review of different nanomaterials used in membranes for various MD and SPMD applications.

4.4.1. Carbon-based materials

Carbon-based materials are expected to be among today's most thoroughly researched additives. Graphene (G), GO, and CNTs have received a lot of attention for water purification processes and treatment, especially pressure-driven membrane processes, and the benefits of using them have been demonstrated by experimental studies [137] and molecular simulations [138]. It is especially crucial for MD applications that carbon-based membranes have high porosity and hydrophobicity. CNTs, G, and GO can influence the water-membrane interface, reducing liquid water permeability while favouring the movement of water vapor molecules [130,139]. These interactions are crucial to membrane function, particularly selectivity and permeability. Fig. 10A shows the CNT mechanisms to prevent liquid water molecule permeation during water-membrane interaction and allow vapor transport through the pores inside the membrane matrix during MD. While Fig. 10B shows how the addition of GO NPs to MD membranes enhances their performance.

The membrane performance of the Psf membrane modified with multi-walled CNT (MWCNT) was investigated by Fahmey et al. [92]. In their study, they enhanced the membrane performance by using a new MD configuration called vacuum enhanced DCMD (VEDCMD) and achieved a permeate flux of 41.58 kg/m²h. According to another study [95], the inclusion of CNTs in the dope solution during the phase inversion process improves flux performance by 12–40 %. Bhadra et al. [88] showed the immobilization of GO on the surface of a PTFE membrane for desalination through DCMD. At 80 °C, the total permeate flow may reach 97 kg/m²h with full salt rejection. In terms of photothermal materials, carbon-based materials, including CB, CNTs, G, GO, reduced GO (rGO), and others, are some of the best-known photothermal materials due to their broad light absorption, high stability, low cost, and lightweight nature. Since the electrons stored loosely in carbon-based compounds have closely spaced energy levels, they absorb broadly over the whole solar spectrum, and the excited electrons relax to their ground state, releasing heat.

The surface of a PVDF nanofibrous membrane was coated with CB NPs using a sprayer to create a rough membrane with localized heating capabilities [110]. The membrane's linked micro/nano channels and multilayer roughness provide omniphobicity, increased vapor permeability, and good light absorption. Through many internal reflections, it could efficiently capture solar energy. Under the illumination of 1.0 kW/m², the membrane surface could be heated from 18.6 to 32.3 °C in 150 s and kept at 41.6 °C for 5 min by the CB NPs-mediated localized heating layer. In addition, to generate effective PMD membranes, other carbon-based nanosheets (NSs) and nanotubes were sprayed onto the surface of the hydrophobic microporous membrane [113]. The fabricated membrane had a CNT-stacked shape. After a few minutes, the membrane demonstrated a steady temperature of over 70 °C under 1.0 kW/m² illumination due to its photothermal conversion efficiency and wide light absorption.

The fabrication of porous structures has proven to be an efficient method for increasing the light absorption of various carbon compounds, the most well-known of which are extremely porous graphene and rGO [141,142]. For example, Ito et al. [143] discovered that the thermal conductivity of a graphene membrane doped with nitrogen could be greatly reduced, resulting in an increased solar evaporation energy efficiency by 13 % when compared to the undoped graphene sample. Aside from man-made structures, at a power density of 12 kW/m, a bi-layered structure built of radially cut wood with a top layer of GO demonstrated an 83 % solar thermal efficiency [144]. A useful supporting layer for solar steam production is wood with a natural vessel structure, as it is considered to have strong optical absorption, low thermal conductivity, hydrophilicity, and abundance.

Although carbon-based materials used in MD applications offer great performance and properties, their alignment is still a source of concern for many researchers. Furthermore, their high cost restricts their commercial applicability, and the health hazards associated with their release into the treated water stream and their stability within the matrix are uncertain.

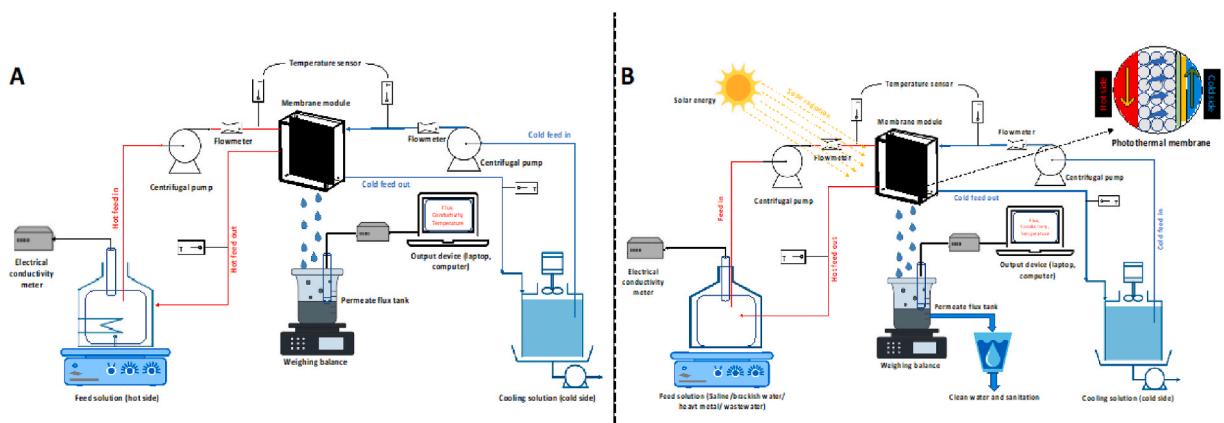


Fig. 11. Comparison of (A) CMD and (B) SPMD.

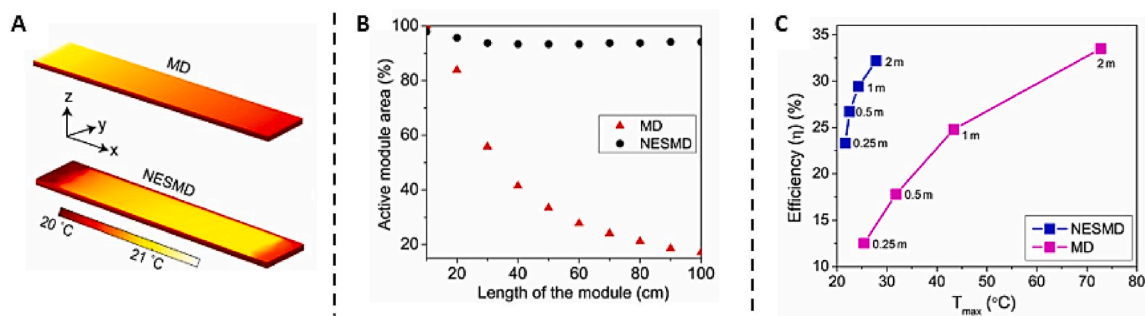


Fig. 12. (A) Calculated temperature distributions at the membrane surface for MD and NESMD; (B) Active membrane area for lengths from 10 to 100 cm and a 10-cm width for MD and NESMD; (C) Efficiency variation with maximum temperature and module length for NESMD and MD. Adopted from Ref. [168]. Copyright, 2017, PNAS.

4.4.2. Metal oxide

Recently, it has been revealed that sphere-like NPs such as ZnO, SiO₂, and titanium dioxide (TiO₂) may be used in MD to induce nano-roughness on membrane surfaces. Hydrophobic TiO₂ nanoparticles functionalized with fluoro-silane were integrated into electrospun membranes to create new membrane designs with superior physicochemical qualities for MD [105]. To evaluate the functionalized TiO₂/PVDF-HFP composite membranes, the membranes were exposed to two days of DCMD to test their selectivity and water vapor flux. All electrospun F-TiO₂/PVDF-HFP membranes showed an anti-wetting feature while retaining a high water flux of 40 L/m²h using a 7.0 wt% NaCl brine as the feed solution when compared to commercial PVDF membranes. In addition, hydrophobic SiO₂ NPs and polydimethylsiloxane (PDMS) were sprayed onto the PVDF membrane to fabricate superhydrophobic membranes with nanostructures for MD [145]. The modified membrane exhibits a lower flux than the unmodified membrane in DCMD experiments with pure water. However, 180-h DCMD experiments with a 25 % NaCl solution show that the modified membrane's permeate flux decreases little when the NaCl rejection rate exceeds 99.99 %, whereas the flux of the unmodified membrane decreases significantly as the rejection rate decreases.

Metal oxides were also used in various research projects, mainly for solar steam generation and in very limited applications for the fabrication of PMD [115]. Light is absorbed in metal oxide semiconductors to produce electron-hole pairs. Solar light, which has more energy than the semiconductor bandgap, would produce electron-hole pairs, which would eventually relax to the band edges and convert the excess energy to heat. Finally, electron-hole pairs in narrow-band gap semiconductors recombine to generate heat [146]. TiO₂ and Ti₂O₃ NPs with high light absorption, for example, have been described and used in solar evaporation and desalination [147, 148]. Huang et al. created titanium nanocages for solar water evaporation that had a high light trapping capacity [149]. A CuCr₂O₄-loaded quartz glass fibre membrane was introduced by Wang et al. in a more recent study as a highly heat-stable solar photothermal material with effective fouling control for evaporation applications and real-world solar distillation [150].

4.4.3. Metals/metal-organic frameworks (MOFs)

MOFs have attracted a lot of interest in MD operations due to their desirable physio-chemical properties, such as high surface area, porosity, and intense capacity to connect organic linkers with inorganic metal centres through coordinate bonds without changing the framework [151,152]. MOFs with clustered centres of iron (Fe), zirconium (Zr), and aluminium (Al) have shown stable properties for water treatment operations in recent studies [153]. Currently, MOFs-incorporated membranes are only employed for VMD and DCMD [100].

According to a few studies, the inclusion of different MOFs can enhance the membrane's wetting resistance and antifouling capabilities by converting its nature from hydrophobic to hydrophilic. Coating 5 wt% Fe-BTC on PVDF membranes, for example, could result in a superhydrophobic PVDF nanofiber membrane for saltwater desalination [101]. According to research, when the composite membrane was used for DCMD, the water CA increased to 138°, the water vapor flux increased, and a 99.9 % of NaCl rejection rate was attained. A new thin-film nanocomposite (TFN) membrane for MD could be created by coating a hydrophobic PVDF membrane with an ultrathin zeolitic imidazolate framework (ZIF-8)/chitosan layer [103]. The results showed that the water permeability increased by 350 %, but the NaCl rejection rate remained at 99.5 %. Furthermore, the presence of the chitosan layer improved antifouling effectiveness.

The plasmon resonance is high in several metals. Hot electrons originate from a collective excitation of the delocalized electrons in metals when the frequency of the incoming light coincides with their oscillation frequency. Through a Joule mechanism, heated electrons vibrate in sync with the electromagnetic field applied [154]. Gold (Au) stands out from its competitors because of its excellent light adsorption tunability, nontoxicity, accessibility to a variety of synthesis methods, and chemical stability [155,156]. Kim et al. demonstrated efficient solar water evaporation by employing flexible thin-film black Au membranes that absorbed 91 % of light between 400 and 500 nm and adiabatic plasmonic nano-focusing to accomplish ultra-broadband light absorption [157]. Self-assembled aluminium (Al) NPs were produced in situ by Zhu et al. in an AAO membrane, and the improved membrane efficiently absorbed a large portion of the solar spectrum (>96 %), resulting in increased saltwater desalination performance [158]. Hu et al.

Table 3
Techno-economic studies on SPMD.

No.	Year	Plant type	System description	Capacity (m ³ /d)	Water Production Cost (US\$/m ³)	Remarks	Ref.
1	2005	Pilot Plant	Economic evaluation of solar-powered AGMD.	65.7	8.95	Nearly 70 % of the water production cost was associated with solar collectors.	[170]
2	2008	Pilot Plant	Economic evaluation of two membrane distillation machines driven by solar energy. Each unit includes a data gathering system, PV panels, spiral AGMD module(s), and flat plate collectors.	0.1 and 0.5	15 for compact system and 18 for large system	The lifespan of the plant and the membrane are important variables in calculating the cost of producing water. As the lifetime of the membrane and/or plant increases, the cost falls.	[171]
3	2012	Pilot Plant	Three stand-alone solar-driven membrane distillation systems (VMD, DCMD, and AGMD).	–	16.02 (VMD), 12.7 (DCMD), 18.26 (AGMD)	DCMD is the most economically effective configuration.	[172]
4	2015	Pilot Plant	Using the currently employed Plate and Frame MD technology, a solar desalination plant was subjected to a techno-economic analysis, with the results being compared to those obtained using fossil fuels.	100	Fossil driven- 8.98, Solar driven- 12.5- 14.12)	There is no significant difference in the water production cost.	[173]
5	2018	Pilot Plant	Performance and cost evaluation study of solar-powered DCMD system.	40.75	0.392	When feed water temperature was raised in the DCMD system, permeate flux and evaporation efficiency increased. However, as input water temperature rise, specific thermal energy consumption dropped.	[174]
6	2018	Modeling	Modeling for economic optimization of a solar driven sweeping gas membrane distillation desalination system	4.15 liters/d/ m ² of collection area	0.085 USD/liter	Membrane modules and solar thermal collectors dominated costs, while thermal and electrical energy storage remained economically unfeasible with current technologies.	[175]
7	2019	Pilot Plant	DCMD with Parabolic Trough Collector	1.14 liters/d/ m ² of collection area	0.021 USD/liter	Solar thermal collectors constituted the largest share of costs, around 25 %, across all configurations and salinity levels. Energy storage was economically unfavourable, leading to the selection of minimal battery and hot water tank sizes. Direct contact membrane distillation incurred higher energy consumption and economic costs compared to other forms.	[176]
8	2020	Modeling	Modeling and performance analysis of a fully solar-powered stand-alone sweeping gas membrane distillation system	4.15 liters/d/ m ² of collection area	0.0183 USD/ liter	Performance comparison with other desalination systems indicates that the system proposed in this paper as a small-scale fully solar powered desalination system is attractive to provide a flexible and reliable fresh water supply for island and coastal households.	[177]
9	2020	Pilot Plant	AGMD Spiral Wound with cooled concentrator PV	19.58 m ³ / year	0.024 USD/liter	The proposed co-generation hybrid system has the capacity to produce fresh potable water of 19.58 m ³ per year and to cut down overall CO ₂ release by about 136.82 kg.	[178]
10	2021	Pilot Plant	The desalination plant utilizes solar energy collected by photovoltaic panels to heat brackish water, employing spiral wound membranes	15.92 liters/ d/m ² of collection area	0.035 USD/liter	The system's specific thermal energy consumption ranged from 90 to 310 kWh/m ³ based on calculations.	[179]
11	2021	Simulation study (Aspen Custom Modeler)	To lower the overall annual cost, the two-stage design approach for SDMD systems is demonstrated in this study using a range of membrane distillation topologies, including AGMD, DCMD, and VMD.	AGMD-28.9, DCMD-31.4, VMD-46.2	AGMD-2.72, DCMD-5.38, and VMD-10.41	The Unit Production Cost of the solar-driven AGMD system can be cut from US\$2.71/m ³ to US\$2.04/m ³ by lowering the membrane unit cost from US\$90/m ³ to US\$36/m ³ .	[180]

(continued on next page)

Table 3 (continued)

No.	Year	Plant type	System description	Capacity (m ³ /d)	Water Production Cost (US\$/m ³)	Remarks	Ref.
12	2022	Pilot Plant	The performance of the pilot plant was analyzed for DCMD & AGMD configuration under various operating conditions and according to onsite weather conditions	10	0.053 USD/liter	An economical evaluation was performed through LCOW comparison in the solar MD pilot plant.	[181]
13	2024	Modeling & simulation	Circulated PGMD module with flat plate solar collectors	6 l/d/m ²	0.016 USD/liter	Pilot hybrid-power 30-stage C-PGMD system, showcasing a remarkable achievement in reducing production costs	[182]

coated the pores of natural wood blocks with Ag, Au, and Pd NPs, which showed excellent stability for more than 144 h and high light absorption capacity (99 %) over a wide wavelength range. In addition, under 10 solar illuminations a high solar conversion efficiency of 85 % was obtained [159].

4.5. Effects of module designs and operational parameters for PMD

The permeate flux of PMD systems is influenced by the designs of membrane modules. The depth of the water layer on the surface of the PMD membrane at the feed side is determined by the design of the membrane module. An increased thickness of the water layer in the feed channel may result in a decrease in the absorption of solar energy by the photothermal layer due to the effects of refraction and scattering [160]. Consequently, this might lead to a reduction in the overall efficiency of the photothermal process. In addition, when the feed solution undergoes light-to-heat conversion on the surface of the PMD membrane, the temperature of the feed rises along the feed flow channel because of the extended heating duration. Hence, the observed temperature disparity is most pronounced on the feed outflow side. Augmenting the dimensions of the membrane module is expected to yield advantageous outcomes in terms of permeate flux [161].

In addition, the photothermal efficiency of the PMD membrane is influenced by the thickness of the photothermal layer and the concentration of the photothermal materials present on its surface. The efficiency of light-to-heat conversion may be improved by including a thicker photothermal layer that possesses a favourable structure, hence facilitating repeated reflections [162]. Nevertheless, a more substantial photothermal layer might potentially impede the permeate fluxes by obstructing the membrane pores and augmenting the barrier to water vapor mass transfer. Researchers showed that an elevated concentration of photothermal materials has the potential to enhance light absorption, resulting in increased light absorption coefficients [163]. They observed that the quasi-steady state surface temperature of the PMD membrane exhibited an increase from 42.4 to 48.0 °C as the concentration of coated CB was raised from 0.2 to 1.0 wt%. The membrane with a lower concentration of CB showed a 9.5 % increase in flux, whereas the membrane with a greater concentration of CB exhibited a 54.9 % increase in membrane flow.

In addition to the membrane properties previously discussed in Section 4.1, the performance of the PMD process can also be influenced by operational circumstances. The primary operating parameters of the PMD process encompass composition, temperature, and feed velocity. The intricate compositions of actual feed solutions have the potential to contaminate and wet the PMD membranes. When the operational temperature of the PMD process is lower, the calcite and gypsum scalants exhibit a tendency to remain dissolved in the feed solution rather than being deposited on the membrane surface [164]. Conversely, the rate at which these scalants precipitate is reduced at lower temperatures, resulting in a delay in the scaling process on the surface of the membrane. Therefore, the PMD process exhibits a reduced degree of membrane scaling compared to CMD processes. The wetting resistance of PMD membrane to surfactant solutions was studied, and it was found that the presence of spherical re-entrant structures inside the photothermal coating layer can enhance PMD membrane wetting resistance [163]. The re-entrant structure has the potential to efficiently stabilize the liquid-vapor interface and inhibit the adsorption of surfactants inside the pores of the membrane, thereby limiting the wetting of the membrane.

Moreover, it is worth noting that the impact of operating circumstances on the permeate side is comparable to that of CMD processes. However, it is important to highlight that the influence of feed velocity on membrane performance is actually opposite for PMD and CMD [161,165]. The PMD process exhibits greater thermal efficiency at lower feed velocities, but the permeate flow in CMD processes may be enhanced at higher feed velocities by mitigating thermal conductivity. A decrease in feed velocity provides an adequate duration for the heating of feed solutions by the PMD membrane, hence creating a greater temperature differential across the membrane. Consequently, this leads to an increased flow of distillate. In contrast, an increase in feed velocity would result in a more rapid transfer of heat from the feed solution layer on the membrane surface to the bulk solution. The PMD system's ability to operate at a low feed velocity would provide a notable advantage over CMD systems.

Furthermore, a study investigated the impact of supplementary feed heating on permeate flux [166]. Prior to entering the PMD membrane module, the feed solution was pre-heated to a temperature range of 30–50 °C. The permeate flow exhibited a positive correlation with the feed temperature, mirroring the behaviour observed in CMD systems. Exposure of the membrane module to light with an intensity of 1 kW/m² resulted in an increase in membrane flux. This observation implies that the PMD process has the potential

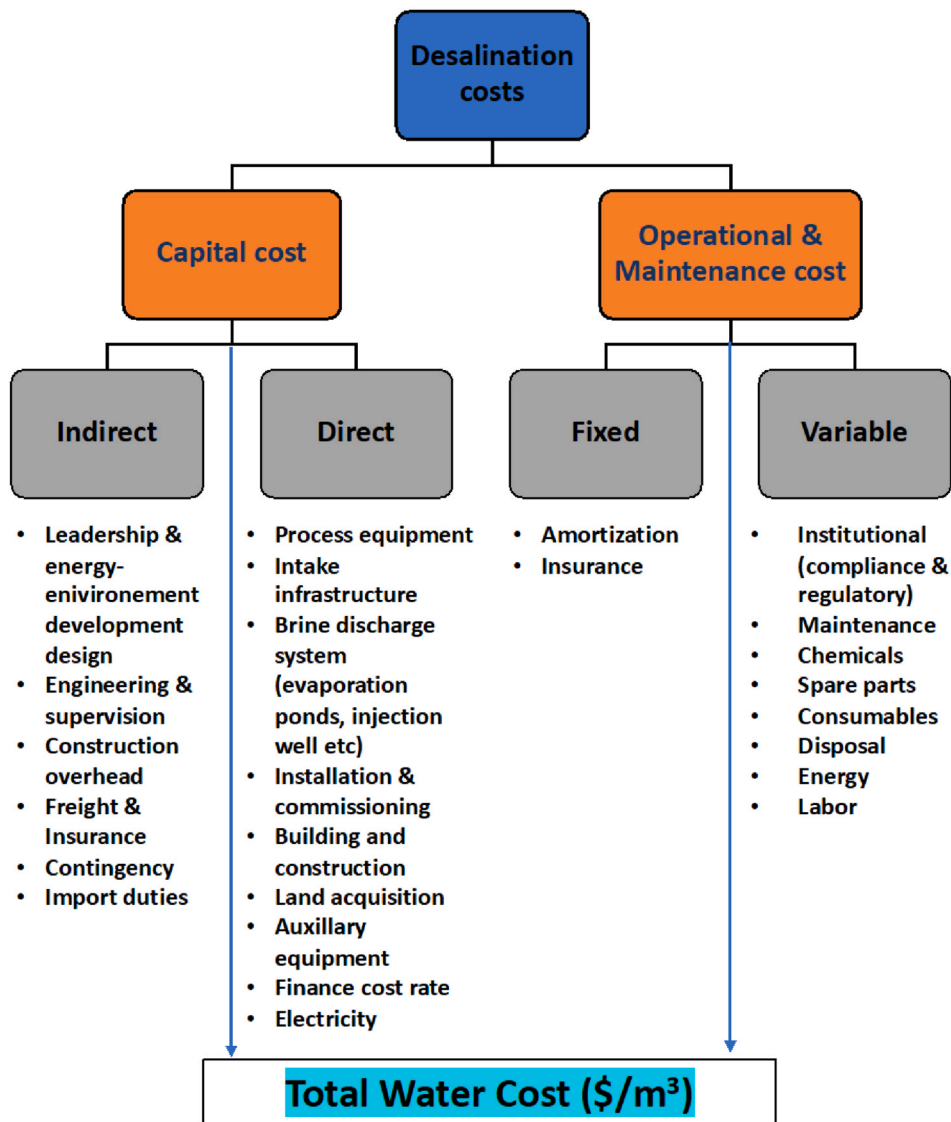


Fig. 13. The diagram of overall desalination cost. Source: Adapted from [183].

to be integrated with auxiliary heating systems to enhance overall performance. One potential avenue for reducing energy usage and cost in PMD systems is through the utilization of wind energy and industrial waste heat.

5. Comparison between CMD and SPMD

With the rising demand for sustainable and energy-efficient desalination methods, the comparison between CMD and SPMD assumes growing significance. When traditional MD technology was compared to a system powered by solar photovoltaic cells, it was shown that DCMD powered by solar energy had lower energy consumption, much higher water output, and thermal efficiency than DCMD powered by electrical energy. Moreover, a DCMD system powered by conventional energy exhibits an 83 % thermal efficiency. In contrast, a comparable system powered by solar energy, specifically through photovoltaic cells, achieves a higher thermal efficiency of 95 % under identical operating conditions but with a distinct driving force source. The substantial flux of solar energy plays a key role in the notable efficiency improvement observed in the solar-operated system compared to its electrical energy-operated counterpart [167]. The comparison between CMD and SPMD is presented in Fig. 11. While CMD relies on external energy sources and is susceptible to TP, PMD utilizes solar energy and photothermal materials to achieve localized heating without using any heaters for the feed water. This mitigates TP, and enhance efficiency, thereby offering potential advantages in terms of energy efficiency, environmental sustainability, and scalability. A detailed mechanism and explanation of TP was explained earlier in the introduction section.

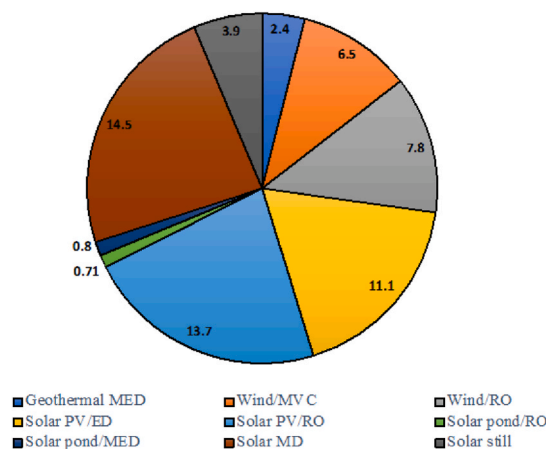
Average Water Production cost (\$/m³)

Fig. 14. Average production cost for desalination technology based on RES. Source: Adapted from Ref. [187].

192

The performance of a standard MD process using pristine PVDF was compared to a nanophotonic-enabled solar MD (NESMD) using CB NPs embedded in an electrospun PVA layer that was applied to a PVDF membrane in Dongare et al. study [168]. As the module size expanded, MD and NESMD performances were evaluated. They discovered that the active membrane area remained high throughout the MD module in the case of the NP-coated membrane, where the transmembrane temperature gradient is positive, but dropped in the case of the uncoated membrane due to increased heat losses from feed to permeate (Fig. 12A and B). As a result, scaling up a NESMD unit should result in a rise in its distillate flow as opposed to MD, where scaling up beyond a certain point does not equate to higher purified water output. Furthermore, the efficiencies of MD and NESMD were compared (Fig. 12C), and the findings demonstrated that NESMD has greater efficiency than MD for modules up to 2 m in length. All these properties point to NESMD as a potential option for community-scale desalination.

¹⁹¹Siefan et al. [169] conducted a life cycle assessment (LCA) to compare the performance of a "large SMADES" SPMD, which desalinates untreated saltwater in Aqaba, Jordan, with a CMD plant. The LCA was performed using SimaPro 9 software, specifically focusing on five distinct scenarios of PV panel types. The purpose was to evaluate and analyse their environmental effects in relation to CMD. The findings of the LCA research primarily centre on the identification of a sustainable MD system in respect to the 22 impact categories. Apart from the global warming potential associated with certain types of PV panels, the findings of this study indicate that the SPMD system, which utilizes a-Si solar panels, is the most favourable choice due to its comparatively reduced environmental footprint in comparison to CMD. Among all other scenarios, it was determined that CMD had the most significant environmental impact. The results of the study indicated that the impact of PV panels on human health, ecological systems, and resource depletion was mitigated by 80 %. In contrast, CMD exhibited a consistent level of 100 % throughout the identical endpoint impact categories. Therefore, it is important to emphasise the need to shift towards more sustainable alternatives that have a positive impact on the environment.

6. Techno-economic studies on SPMD

The economic viability of separation technologies based on membranes used for treating wastewater, brackish water, seawater or saline/hypersaline water, groundwater, and food processing (vegetable and fruit juice concentration) must be accessed through techno-economic analysis. Membrane-based separation technologies can run on a variety of energy sources, such as fossil fuels like natural gas, crude oil, and coal, as well as renewable sources like wind energy hydroelectric power, geothermal energy, and solar energy. Based on their investment (operation cost and capital costs), water production costs were evaluated for any chemical process like solar-powered membrane distillation system. It is crucial to note that different types of membrane-based separation technologies have different cost estimates for energy consumption and water output depending on the site, differences in the boundaries of the system, site-specific salt content, economic indicators unique to the site location, and plant lifespan. So far, very few studies have been presented in the literature that deal with the cost of producing water and the energy consumption of SPMD, which are listed in Table 3.

In terms of energy consumption, MD is known for its low energy requirements, particularly when compared to other thermal desalination technologies such as multi-stage flash (MSF) and multi-effect distillation (MED). MD typically requires energy inputs in the range of 10–40 kWh/ m³, which is significantly lower than MSF and MED (energy inputs in the range of 50–80 kWh/ m³ and 25–35 kWh/ m³, respectively). However, when compared to other membrane-based technologies such as RO, MD typically requires higher energy inputs. RO typically requires energy inputs in the range of 3–4 kWh/ m³, which is significantly lower than MD. However, MD

has several advantages over RO, such as its ability to handle feedwater with high salinity and fouling potential, making it a more attractive option for certain applications.

The cost of traditional desalination methods comprises of several costs as shown in Fig. 13. However, factors such as market competition, new processes, and material improvements are contributing to lower costs in thermal desalination processes. Technological advancements are expected to further reduce equipment costs and overall plant costs. As a result, desalination is becoming a practical and cost-competitive option for providing drinkable water. However, the costs of pre-treatment and post-treatment processes still impact the overall cost of desalinated water. The increasing costs of traditional energy production could offset the cost reduction trend, but the integration of renewable energy sources (RES) is expected to change this projection soon.

Assessing the average cost of water production is crucial for evaluating the feasibility and economic viability of different technologies. For instance, the average cost of producing water from seawater using traditional desalination methods is approximately \$1.4/m³ for MSF technology, \$1/m³ for MED, and \$0.5/m³ for RO. Estimates for CMD vary widely, ranging from \$0.5/m³ to over \$15/m³ of purified water. Discrepancies in cost estimates can be attributed to factors such as plant capacity, feed water salinity, and energy sources utilized [184,185]. On the other hand, SPMD systems entail initial setup costs for solar panels and infrastructure, but offer potential long-term savings on energy expenses, with the cost per cubic meter ranging from \$0.30 to \$14.50. This data underscores the importance of comprehensive cost analyses in determining the most cost-effective approach for water desalination projects. Fig. 14 shows various desalination technologies powered by RES. In conclusion, MD may not be the most economic membrane-based technology, however, its low energy requirements relative to other thermal desalination technologies make it a promising option for water purification, particularly in situations where waste heat or solar energy is available [186].

7. Future perspective of SPMD

Water and energy are crucial for socio-economic development in many nations throughout the world, especially in Africa and Asia, and they also play a significant role in sustainable development. Both sustainable energy production and water purification are heavily dependent on membrane-based technologies, either alone or in conjunction with other membrane-based processes. To make the process more affordable, manageable, and suitable for industrial applications, these technologies could be integrated with renewable energy sources, including geothermal, hydropower, wind, and solar energy (photovoltaic panels and thermal collectors). SPMD process design is becoming more popular on a global scale, especially for water treatment and desalination, as it is an appealing and new water reclamation method.

This review offers significant recommendations for the future that could be addressed by advancing the SPMD desalination process and removing barriers, and these are noted below.

- More research is required to create extremely resilient photothermal materials with suitable functionalities for incorporating them into membrane composites.
- Investigations need to be performed on the scalability of SPMD systems with effective latent heat recovery, little heat loss, and compact designs. Finally, the economic and ecological benefits must be thoroughly considered before the SPMD system can be widely used to provide a safe and economical water supply.
- Furthermore, SPMD membrane designs must consider the kinetics and behaviors of thermal diffusion, vapor generation, and light adsorption. Real-time monitoring and simulation may be useful methods to gain insight into the underlying concepts.
- As most membrane materials are polymers, prolonged exposure to sunlight can cause them to break down and fail. Therefore, it is important to investigate the durability and stability of the membrane.
- In addition to scalability, the affordability of SPMD membranes and systems is essential to determining how competitive this technology is.
- The underlying molecular mechanism has not been discovered to explain why the addition of the MOFs and other materials can increase membrane flux, how the dense-layer coating prevents surfactants and organics from wetting the membrane, or how the water or organics move across the dense layer as vapor, liquid, or molecules.

Table 4
Comparative analysis of CMD and SPMD based on different aspects.

Aspect	Conventional Membrane Distillation	Solar-powered Membrane Distillation
Strengths	<ul style="list-style-type: none"> - Established technology - High energy efficiency - Consistent performance - Well understood process 	<ul style="list-style-type: none"> - Utilizes abundant solar energy - Environmentally friendly - Potential for decentralized systems - Low operating cost
Limitations	<ul style="list-style-type: none"> - Reliance on external energy - High energy consumption - Expensive infrastructure - Environmental concern (eg. Brine discharge) 	<ul style="list-style-type: none"> - Intermittent energy source - Weather-dependent performance - Limited scalability - Variable water production
Scale of Testing	Usually tested at commercial scale	Typically tested at pilot or small-scale
Cost characteristics	Higher operating costs, lower initial investment	Lower operating costs, higher initial investment
Efficiency and Productivity	Generally high and consistent	Variable depending on weather conditions
Aim to increase deployment	Improve efficiency and reliability	Increase sustainability and access to clean water

- Self-cleaning membranes, a great concept, have the potential to revolutionize anti-fouling membranes, which can be applied in commercial SPMD applications and further the understanding of SPMD membranes.
- Future research is necessary to ascertain whether novel MD process configurations have the potential to substantially reduce the environmental footprint by raising average water flows at the module level without significantly compromising energy efficiency.
- The most promising industrial use for solar-powered MD is the treatment of produced water from shale oil and unconventional gas extraction, natural gas exploration, and oilfields.
- Large-scale solar water treatment facilities are not currently being built, but they could present a chance to lower overall capital costs. The investigation of the upgrade and its commercial viability, therefore, calls for more demonstration and simulation research.

The innovative conclusions from these investigations demonstrate the significance of MD supported by solar energy for desalination procedures. Numerous design plans have demonstrated significant advances in different membrane distillation modules. Additionally, those findings hold promise for more in-depth investigation and may be appropriate for practical applications.

8. Conclusion

In conclusion, this comprehensive review aims to provide a deep understanding of both CMD and SPMD systems, exploring their configurations, mechanisms, and associated challenges. Additionally, various methods for membrane fabrication and techniques to enhance MD performance have been examined. The prospects of SPMD were discussed, shedding light on barriers to commercialization such as temperature and concentration polarization, and membrane design intricacies. While solar-integrated desalination technologies are in the research and development phase, intensifying efforts in this field is imperative for scientific and technological advancement.

Direct SPMD desalination technology presents a promising solution for small-scale applications, optimizing the utilization of solar energy. Incorporating solar absorption and MD into a single, compact module efficiently reduces heat loss, particularly in comparison to indirect configurations. By employing photothermal heating on the membrane surface, it becomes possible to enhance and maintain the feed/membrane interface surface temperature, thereby reducing TP. However, achieving optimal desalination performance requires consideration of various factors, including the characteristics of photothermal materials (such as chemical stability, long-term durability, anti-fouling properties, toxicity, and cost), operating conditions (such as flow rate, initial feed temperature, and salinity), and system design (including SPMD configuration, membrane type, and module length). For instance, unlike CMD processes, enlarging the module size in SPMD or reducing the feed flow rate can enhance water production by prolonging the contact time between the membrane as a heating source and the feed. Conversely, raising the inlet feed temperature above that of the photothermal membrane surface may diminish the benefits of the photothermal material as a solar absorber. However, it was noticed that the photothermal materials used in SPMD systems are similar to the materials used in CMD systems. Both systems mainly desire materials with characteristics, such as mechanical and chemical stability, hydrophobic surfaces for feed-distillate separation, and high porosity for vapor diffusion. In addition to the aforementioned characteristics, characteristics such as high photothermal conversion efficiency, multiple light scattering and trapping, and broadband solar absorption must be evaluated and taken into account when selecting SPMD materials. As a result, more efforts are required to produce extremely durable photothermal materials with necessary properties for incorporation into SPMD systems. Moreover, despite the observed quick advancement in SPMD research activities, many investigations are focused on modeling and simulation. There is an urgent need to bridge the theoretical and experimental gap to get solar MD closer to commercialization. Therefore, for enhanced improvement, a pilot-scale plant's long-term operational experience is essential. Overall, the nanoparticle-modified membranes have proven to be highly effective in addressing many problems associated with MD. Mainly, the carbon-based NPs are the ones extensively used for both conventional and solar MD, due to their special characteristics.

Table 4 summarizes the strengths and limitations of solar-powered desalination compared to conventional methods. Careful consideration of the aspects mentioned alongside technical feasibility assessments is crucial for evaluating the overall viability and potential benefits of adopting SPMD and photothermal technologies for water treatment applications.

Data availability

Data included in article/supp. material/referenced in the article is available.

CRediT authorship contribution statement

Ahmad S. Jawed: Writing – original draft, Investigation, Formal analysis, Data curation, Conceptualization. **Lobna Nassar:** Writing – original draft, Investigation, Formal analysis, Data curation, Conceptualization. **Hanaa M. Hegab:** Writing – review & editing, Supervision, Investigation, Formal analysis, Data curation, Conceptualization. **Riaan van der Merwe:** Writing – review & editing. **Faisal Al Marzooqi:** Writing – review & editing, Supervision. **Fawzi Banat:** Writing – review & editing, Supervision. **Shadi W. Hasan:** Writing – review & editing, Supervision, Funding acquisition, Conceptualization.

Declaration of competing interest

The authors declare that they have no known competing financial interests or personal relationships that could have appeared to influence the work reported in this paper.

Acknowledgments

This research is supported by ASPIRE, the technology program management pillar of Abu Dhabi's Advanced Technology Research Council (ATRC), via the ASPIRE VRI (Virtual Research Institute) Award. The authors would also like to thank the Center for Membranes and Advanced Water Technology (CMAT) at Khalifa University for their support (RC2-2018-009).

References

- [1] C. Zhang, H.Q. Liang, Z.K. Xu, Z. Wang, Harnessing solar-driven photothermal effect toward the water–energy nexus, *Adv. Sci.* 6 (2019) 1900883, <https://doi.org/10.1002/ADVS.201900883>.
- [2] N.A. Ahmad, P.S. Goh, L.T. Yogarathinam, A.K. Zulhairun, A.F. Ismail, Current advances in membrane technologies for produced water desalination, *Desalination* 493 (2020), <https://doi.org/10.1016/J.DESAL.2020.114643>.
- [3] M. Elimelech, W.A. Phillip, The future of seawater desalination: energy, technology, and the environment, *Science* (1979) 333 (2011) 712–717, https://doi.org/10.1126/SCIENCE.1200488/SUPPL_FILE/ELIMELECH.SOM.PDF.
- [4] M. Hameed, H. Moradkhani, A. Ahmadipour, H. Moftakhari, P. Abbaszadeh, A. Alipour, A review of the 21st Century challenges in the food-energy-water Security in the Middle East, *Water* 11 (2019) 682, <https://doi.org/10.3390/W11040682>, 682 11 (2019).
- [5] Y.R. Chen, R. Xin, X. Huang, K. Zuo, K.L. Tung, Q. Li, Wetting-resistant photothermal nanocomposite membranes for direct solar membrane distillation, *J Memb Sci* 620 (2021) 118913, <https://doi.org/10.1016/J.MEMSCI.2020.118913>.
- [6] F.E. Ahmed, R. Hashaikh, N. Hilal, Solar powered desalination – technology, energy and future outlook, *Desalination* 453 (2019) 54–76, <https://doi.org/10.1016/j.desal.2018.12.002>.
- [7] Y. Liao, R. Wang, A.G. Fane, Fabrication of bioinspired composite nanofiber membranes with robust superhydrophobicity for direct contact membrane distillation, *Environ. Sci. Technol.* 48 (2014) 6335–6341, https://doi.org/10.1021/ES405795S/SUPPL_FILE/ES405795S_SI_001.PDF.
- [8] B. van der Bruggen, Integrated membrane separation processes for recycling of valuable wastewater streams: Nanofiltration, membrane distillation, and membrane Crystallizers Revisited, *Ind. Eng. Chem. Res.* 52 (2013) 10335–10341, <https://doi.org/10.1021/IE302880A>.
- [9] K. Zuo, W. Wang, A. Deshmukh, S. Jia, H. Guo, R. Xin, M. Elimelech, P.M. Ajayan, J. Lou, Q. Li, Multifunctional nanocoated membranes for high-rate electrothermal desalination of hypersaline waters, *Nat. Nanotechnol.* (15) (2020) 1025–1032, <https://doi.org/10.1038/s41565-020-00777-0>, 2020 15:12.
- [10] A. Anvari, A. Azimi Yancheshme, K.M. Kekre, A. Ronen, State-of-the-art methods for overcoming temperature polarization in membrane distillation process: a review, *J Memb Sci* 616 (2020) 118413, <https://doi.org/10.1016/J.MEMSCI.2020.118413>.
- [11] Y. Elhenawy, N.A.S. Elminshawy, M. Bassouni, A. Alhathal Alanezi, E. Drioli, Experimental and theoretical investigation of a new air gap membrane distillation module with a corrugated feed channel, *J Memb Sci* 594 (2020) 117461, <https://doi.org/10.1016/J.MEMSCI.2019.117461>.
- [12] M. Albeirutty, N. Turkmen, S. Al-Sharif, S. Bouguecha, A. Malik, O. Faruki, A. Cipollina, M. Ciofalo, G. Micale, An experimental study for the characterization of fluid dynamics and heat transport within the spacer-filled channels of membrane distillation modules, *Desalination* 430 (2018) 136–146, <https://doi.org/10.1016/J.DESAL.2017.12.043>.
- [13] A. Politano, P. Argurio, G. Di Profio, V. Sanna, A. Cupolillo, S. Chakraborty, H.A. Arafat, E. Curcio, Photothermal membrane distillation for seawater desalination, *Adv. Mater.* 29 (2017) 1603504, <https://doi.org/10.1002/ADMA.201603504>.
- [14] Y. Zhou, R.S.J. Tol, Evaluating the costs of desalination and water transport, *Water Resour. Res.* 41 (2005) 1–10, <https://doi.org/10.1029/2004WR003749>.
- [15] P.W. Bohn, M. Elimelech, J.G. Georgiadis, B.J. Marinás, A.M. Mayes, A.M. Mayes, Science and technology for water purification in the coming decades, *Nanoscience and Technology: A Collection of Reviews from Nature Journals* (2009) 337–346, https://doi.org/10.1142/9789814287005_0035.
- [16] A.E. Jansen, J.W. Assink, J.H. Hanemaaijer, J. van Medevoort, E. van Sonsbeek, Development and pilot testing of full-scale membrane distillation modules for deployment of waste heat, *Desalination* 323 (2013) 55–65, <https://doi.org/10.1016/J.DESAL.2012.11.030>.
- [17] A. Deshmukh, C. Boo, V. Karanikola, S. Lin, A.P. Straub, T. Tong, D.M. Warsinger Ab, M. Elimelech, Membrane distillation at the water-energy nexus: limits, opportunities, and challenges, *Cite This: energy, Environ. Sci.* 11 (2018) 1177, <https://doi.org/10.1039/c8ee00291f>.
- [18] X. Tong, X. Wang, S. Liu, H. Gao, R. Hao, Y. Chen, Low-grade waste heat recovery via an Osmotic heat engine by using a Freestanding graphene oxide membrane, *ACS Omega* 3 (2018) 15501–15509, https://doi.org/10.1021/ACSOMEGA.8B02101/SUPPL_FILE/AO8B02101_SI_001.PDF.
- [19] X. Tong, X. Wang, S. Liu, H. Gao, R. Hao, Y. Chen, Low-grade waste heat recovery via an Osmotic heat engine by using a Freestanding graphene oxide membrane, *ACS Omega* 3 (2018) 15501–15509, https://doi.org/10.1021/ACSOMEGA.8B02101/SUPPL_FILE/AO8B02101_SI_001.PDF.
- [20] U. Manufacturing, Energy Use, loss and opportunities analysis. www.eere.energy.gov/industry/energy_systems, 2004. (Accessed 15 July 2022).
- [21] A. Deshmukh, C. Boo, V. Karanikola, S. Lin, A.P. Straub, T. Tong, D.M. Warsinger, M. Elimelech, Membrane distillation at the water-energy nexus: limits, opportunities, and challenges, *Energy Environ. Sci.* 11 (2018) 1177–1196, <https://doi.org/10.1039/C8EE00291F>.
- [22] E. Guillén-Burrieza, J. Blanco, G. Zaragoza, D.C. Alarcón, P. Palenzuela, M. Ibarra, W. Gernjak, Experimental analysis of an air gap membrane distillation solar desalination pilot system, *J Memb Sci* 379 (2011) 386–396, <https://doi.org/10.1016/J.MEMSCI.2011.06.009>.
- [23] A. Hafidz, E.D. Kerme, I. Wazeer, Y. Khalid, A. Ajbar, S.M. Al-Zahrani, Design and fabrication of a portable and hybrid solar-powered membrane distillation system, *J. Clean. Prod.* 133 (2016) 631–647, <https://doi.org/10.1016/J.JCLEPRO.2016.05.127>.
- [24] M.I. Soomro, W.S. Kim, Y.D. Kim, Performance and cost comparison of different concentrated solar power plants integrated with direct-contact membrane distillation system, *Energy Convers. Manag.* 221 (2020), <https://doi.org/10.1016/J.ENCONMAN.2020.113193>.
- [25] A. Bamasag, E. Almatrafi, T. Alqahtani, P. Phelan, M. Ullah, M. Mustakeem, M. Obaid, N. Ghaffour, Recent advances and future prospects in direct solar desalination systems using membrane distillation technology, *J. Clean. Prod.* 385 (2023) 135737, <https://doi.org/10.1016/J.JCLEPRO.2022.135737>.
- [26] V.K. Chauhan, S.K. Shukla, J.V. Tirkey, P.K. Singh Rathore, A comprehensive review of direct solar desalination techniques and its advancements, *J. Clean. Prod.* 284 (2021) 124719, <https://doi.org/10.1016/J.JCLEPRO.2020.124719>.
- [27] A.E. Kabeel, S.A. El-Agouz, Review of researches and developments on solar stills, *Desalination* 276 (2011) 1–12, <https://doi.org/10.1016/J.DESAL.2011.03.042>.
- [28] K. Kalidasa Murugavel, P. Anburaj, R. Samuel Hanson, T. Elango, Progresses in inclined type solar stills, *Renew. Sustain. Energy Rev.* 20 (2013) 364–377, <https://doi.org/10.1016/J.RSER.2012.10.047>.
- [29] T. Rajaseenivasan, T. Elango, K. Kalidasa Murugavel, Comparative study of double basin and single basin solar stills, *Desalination* 309 (2013) 27–31, <https://doi.org/10.1016/J.DESAL.2012.09.014>.
- [30] T. Arunkumar, H.W. Lim, S.J. Lee, A review on efficiently integrated passive distillation systems for active solar steam evaporation, *Renew. Sustain. Energy Rev.* 155 (2022) 111894, <https://doi.org/10.1016/J.RSER.2021.111894>.
- [31] A. Bamasag, F.A. Essa, Z.M. Omara, E. Bahgat, A.O. Alsaiani, H. Abulkhair, R.A. Alsulami, A.H. Elsheikh, Machine learning-based prediction and augmentation of dish solar distiller performance using an innovative convex stepped absorber and phase change material with nanoadditives, *Process Saf. Environ. Protect.* 162 (2022) 112–123, <https://doi.org/10.1016/J.PSEP.2022.03.052>.

- [32] E.K. Summers, J.H. Lienhard, Experimental study of thermal performance in air gap membrane distillation systems, including the direct solar heating of membranes, *Desalination* 330 (2013) 100–111, <https://doi.org/10.1016/J.DESAL.2013.09.023>.
- [33] T.C. Chen, C.D. Ho, Immediate assisted solar direct contact membrane distillation in saline water desalination, *J Memb Sci* 358 (2010) 122–130, <https://doi.org/10.1016/J.MEMSCI.2010.04.037>.
- [34] Q. Ma, A. Ahmadi, C. Cabassud, Direct integration of a vacuum membrane distillation module within a solar collector for small-scale units adapted to seawater desalination in remote places: design, modeling & evaluation of a flat-plate equipment, *J Memb Sci* 564 (2018) 617–633, <https://doi.org/10.1016/J.MEMSCI.2018.07.067>.
- [35] T.C. Chen, C.D. Ho, Immediate assisted solar direct contact membrane distillation in saline water desalination, *J Memb Sci* 358 (2010) 122–130, <https://doi.org/10.1016/J.MEMSCI.2010.04.037>.
- [36] Q. Ma, A. Ahmadi, C. Cabassud, Optimization and design of a novel small-scale integrated vacuum membrane distillation - solar flat-plate collector module with heat recovery strategy through heat pumps, *Desalination* 478 (2020) 114285, <https://doi.org/10.1016/J.DESAL.2019.114285>.
- [37] S. Soukane, N. Ghaffour, Showerhead feed distribution for optimized performance of large scale membrane distillation modules, *J Memb Sci* 618 (2021) 118664, <https://doi.org/10.1016/J.MEMSCI.2020.118664>.
- [38] W. Wang, Y. Shi, C. Zhang, S. Hong, L. Shi, J. Chang, R. Li, Y. Jin, C. Ong, S. Zhuo, P. Wang, Simultaneous production of fresh water and electricity via multistage solar photovoltaic membrane distillation, *Nat. Commun.* 10 (2019) 1–9, <https://doi.org/10.1038/s41467-019-10817-6>, 2019 10:1.
- [39] G. Antonetto, M. Morciano, M. Alberghini, G. Malgaroli, A. Ciocia, L. Bergamasco, F. Spertino, M. Fasano, Synergistic freshwater and electricity production using passive membrane distillation and waste heat recovered from camouflaged photovoltaic modules, *J. Clean. Prod.* 318 (2021) 128464, <https://doi.org/10.1016/J.JCLEPRO.2021.128464>.
- [40] S. Soukane, H.S. Son, M. Mustakeem, M. Obaid, A. Alpatova, A. Qamar, Y. Jin, N. Ghaffour, Materials for energy conversion in membrane distillation localized heating: review, analysis and future perspectives of a paradigm shift, *Renew. Sustain. Energy Rev.* 167 (2022) 112702, <https://doi.org/10.1016/J.RSER.2022.112702>.
- [41] E.K. Summers, J.H. Lienhard, Experimental study of thermal performance in air gap membrane distillation systems, including the direct solar heating of membranes, *Desalination* 330 (2013) 100–111, <https://doi.org/10.1016/J.DESAL.2013.09.023>.
- [42] A. Politano, P. Argurio, G. Di Profio, V. Sanna, A. Cupolillo, S. Chakraborty, H.A. Arafat, E. Curcio, Photothermal membrane distillation for seawater desalination, *Adv. Mater.* 29 (2017) 1603504, <https://doi.org/10.1002/ADMA.201603504>.
- [43] X. Wu, Q. Jiang, D. Ghim, S. Singamaneni, Y.S. Jun, Localized heating with a photothermal polydopamine coating facilitates a novel membrane distillation process, *J Mater Chem A Mater* 6 (2018) 18799–18807, <https://doi.org/10.1039/C8TA05738A>.
- [44] M.U. Farid, J.A. Kharraz, A.K. An, Plasmonic titanium nitride nano-enabled membranes with high structural stability for efficient photothermal desalination, *ACS Appl. Mater. Interfaces* 13 (2021) 3805–3815, https://doi.org/10.1021/ACSAMI.0C17154/SUPPL_FILE/AM0C17154_SI_001.PDF.
- [45] X. Wu, S. Cao, D. Ghim, Q. Jiang, S. Singamaneni, Y.S. Jun, A thermally engineered polydopamine and bacterial nanocellulose bilayer membrane for photothermal membrane distillation with bactericidal capability, *Nano Energy* 79 (2021) 105353, <https://doi.org/10.1016/J.NANOEN.2020.105353>.
- [46] W. Li, L. Deng, H. Huang, J. Zhou, Y. Liao, L. Qiu, H. Yang, L. Yao, Janus photothermal membrane as an energy generator and a mass-transfer Accelerator for high-efficiency solar-driven membrane distillation, *ACS Appl. Mater. Interfaces* 13 (2021) 26861–26869, https://doi.org/10.1021/ACSAMI.1C01072/SUPPL_FILE/AM1C01072_SI_001.PDF.
- [47] V.G. Gude, N. Nirmalakkhandan, S. Deng, Renewable and sustainable approaches for desalination, *Renew. Sustain. Energy Rev.* 14 (2010) 2641–2654, <https://doi.org/10.1016/J.RSER.2010.06.008>.
- [48] H.M. Qiblawey, F. Banat, Solar thermal desalination technologies, *Desalination* 220 (2008) 633–644, <https://doi.org/10.1016/J.DESAL.2007.01.059>.
- [49] S.A. Kalogirou, Solar thermal collectors and applications, *Prog. Energy Combust. Sci.* 30 (2004) 231–295, <https://doi.org/10.1016/J.PECS.2004.02.001>.
- [50] V. Velmurugan, K. Srithar, Prospects and scopes of solar pond: a detailed review, *Renew. Sustain. Energy Rev.* 12 (2008) 2253–2263, <https://doi.org/10.1016/J.RSER.2007.03.011>.
- [51] Jenny Lindblom, Solar thermal technologies for seawater desalination: state of the art, *Renewable Energy Systems*, Luleå University of Technology, Sweden (n.d.), https://www.researchgate.net/publication/228401141_Solar_thermal_technologies_for_seawater_desalination_state_of_the_art. (Accessed 16 July 2022).
- [52] R. Nagaraj, Renewable energy based small hybrid power system for desalination applications in remote locations, in: *India International Conference on Power Electronics, IICPE, 2012*, <https://doi.org/10.1109/IICPE.2012.6450437>.
- [53] V.G. Gude, N. Nirmalakkhandan, S. Deng, Renewable and sustainable approaches for desalination, *Renew. Sustain. Energy Rev.* 14 (2010) 2641–2654, <https://doi.org/10.1016/J.RSER.2010.06.008>.
- [54] A. Lamei, P. van der Zaag, E. von Münch, Impact of solar energy cost on water production cost of seawater desalination plants in Egypt, *Energy Pol.* 36 (2008) 1748–1756, <https://doi.org/10.1016/J.ENPOL.2007.12.026>.
- [55] S. Al-Obaidani, F. Macedonio, G. di Profio, H. Al-Hinai, E. Curcio, F. Macedonio, G. di Profio, E. Drioli, Matching-Materials Technologies for performance improvement of Cooling Systems in Power Plants View project Potential of membrane distillation in seawater desalination: thermal efficiency, sensitivity study and cost estimation, *Article in Journal of Membrane Science* 323 (2008) 85–98, <https://doi.org/10.1016/j.memsci.2008.06.006>.
- [56] N. Tang, Q. Jia, H. Zhang, J. Li, S. Cao, Preparation and morphological characterization of narrow pore size distributed polypropylene hydrophobic membranes for vacuum membrane distillation via thermally induced phase separation, *Desalination* 256 (2010) 27–36, <https://doi.org/10.1016/J.DESAL.2010.02.024>.
- [57] H. Zhu, H. Wang, F. Wang, Y. Guo, H. Zhang, J. Chen, Preparation and properties of PTFE hollow fiber membranes for desalination through vacuum membrane distillation, *J Memb Sci* 446 (2013) 145–153, <https://doi.org/10.1016/J.MEMSCI.2013.06.037>.
- [58] S. Devi, P. Ray, K. Singh, P.S. Singh, Preparation and characterization of highly micro-porous PVDF membranes for desalination of saline water through vacuum membrane distillation, *Desalination* 346 (2014) 9–18, <https://doi.org/10.1016/J.DESAL.2014.05.004>.
- [59] M.C. García-Payo, M.A. Izquierdo-Gil, C. Fernández-Pineda, Air gap membrane distillation of aqueous alcohol solutions, *J Memb Sci* 169 (2000) 61–80, [https://doi.org/10.1016/S0376-7388\(99\)00326-9](https://doi.org/10.1016/S0376-7388(99)00326-9).
- [60] M. Essalhi, M. Khayet, Self-sustained webs of polyvinylidene fluoride electrospun nanofibers at different electrospinning times: 1. Desalination by direct contact membrane distillation, *J Memb Sci* 433 (2013) 167–179, <https://doi.org/10.1016/J.MEMSCI.2013.01.023>.
- [61] K. Schneider, W. Hölz, R. Wollbeck, S. Ripperger, Membranes and modules for transmembrane distillation, *J Memb Sci* 39 (1988) 25–42, [https://doi.org/10.1016/S0376-7388\(00\)80992-8](https://doi.org/10.1016/S0376-7388(00)80992-8).
- [62] A.C.M. Franken, J.A.M. Nolten, M.H.V. Mulder, D. Bargeman, C.A. Smolders, Wetting criteria for the applicability of membrane distillation, *J Memb Sci* 33 (1987) 315–328, [https://doi.org/10.1016/S0376-7388\(00\)80288-4](https://doi.org/10.1016/S0376-7388(00)80288-4).
- [63] M. Khayet, T. Matsuura, Preparation and characterization of polyvinylidene fluoride membranes for membrane distillation, *Ind. Eng. Chem. Res.* 40 (2001) 5710–5718, <https://doi.org/10.1021/IE010553Y>.
- [64] S. Adnan, M. Hoang, H. Wang, Z. Xie, Commercial PTFE membranes for membrane distillation application: effect of microstructure and support material, *Desalination* 284 (2012) 297–308, <https://doi.org/10.1016/J.DESAL.2011.09.015>.
- [65] A. Alkhudhiri, N. Darwish, N. Hilal, Membrane distillation: a comprehensive review, *Desalination* 287 (2012) 2–18, <https://doi.org/10.1016/J.DESAL.2011.08.027>.
- [66] B.S. Lalia, E. Guillen-Burrieza, H.A. Arafat, R. Hashaikeh, Fabrication and characterization of polyvinylidene fluoride-co-hexafluoropropylene (PVDF-HFP) electrospun membranes for direct contact membrane distillation, *J Memb Sci* 428 (2013) 104–115, <https://doi.org/10.1016/J.MEMSCI.2012.10.061>.
- [67] M.S. El-Bourawi, Z. Ding, R. Ma, M. Khayet, A framework for better understanding membrane distillation separation process, *J Memb Sci* 285 (2006) 4–29, <https://doi.org/10.1016/J.MEMSCI.2006.08.002>.
- [68] A.O. Imdakm, T. Matsuura, A Monte Carlo simulation model for membrane distillation processes: direct contact (MD), *J Memb Sci* 237 (2004) 51–59, <https://doi.org/10.1016/J.MEMSCI.2004.03.005>.

- [69] A.O. Imdakm, T. Matsuura, Simulation of heat and mass transfer in direct contact membrane distillation (MD): the effect of membrane physical properties, *J Memb Sci* 262 (2005) 117–128, <https://doi.org/10.1016/J.MEMSCI.2005.05.026>.
- [70] M. Khayet, A. Velázquez, J.I. Mengual, Modelling mass transport through a porous partition: effect of pore size distribution, *J. Non-Equilibrium Thermodyn.* 29 (2004) 279–299, <https://doi.org/10.1515/JNETDY.2004.055>.
- [71] H.Y. Wu, R. Wang, R.W. Field, Direct contact membrane distillation: an experimental and analytical investigation of the effect of membrane thickness upon transmembrane flux, *J Memb Sci* 470 (2014) 257–265, <https://doi.org/10.1016/J.MEMSCI.2014.06.002>.
- [72] L. Eykens, I. Hitsov, K. De Sitter, C. Dotremont, L. Pinoy, I. Nopens, B. Van der Bruggen, Influence of membrane thickness and process conditions on direct contact membrane distillation at different salinities, *J Memb Sci* 498 (2016) 353–364, <https://doi.org/10.1016/J.MEMSCI.2015.07.037>.
- [73] J. Phattaranawik, R. Jiratananon, A.G. Fane, Heat transport and membrane distillation coefficients in direct contact membrane distillation, *J Memb Sci* 212 (2003) 177–193, [https://doi.org/10.1016/S0376-7388\(02\)00498-2](https://doi.org/10.1016/S0376-7388(02)00498-2).
- [74] M. Khayet, T. Matsuura, J.I. Mengual, M. Qtaishat, Design of novel direct contact membrane distillation membranes, *Desalination* 192 (2006) 105–111, <https://doi.org/10.1016/J.DESAL.2005.06.047>.
- [75] B.B. Ashoor, S. Mansour, A. Giwa, V. Dufour, S.W. Hasan, Principles and applications of direct contact membrane distillation (DCMD): a comprehensive review, *Desalination* 398 (2016) 222–246, <https://doi.org/10.1016/J.DESAL.2016.07.043>.
- [76] M. Rezaei, D.M. Warsinger, J.H. Lienhard V, M.C. Duke, T. Matsuura, W.M. Samhaber, Wetting phenomena in membrane distillation: mechanisms, reversal, and prevention, *Water Res.* 139 (2018) 329–352, <https://doi.org/10.1016/J.WATRES.2018.03.058>.
- [77] D. Rice, S.J. Ghadimi, A.C. Barrios, S. Henry, W.S. Walker, Q. Li, F. Perreault, Scaling resistance in Nanophotonics-enabled solar membrane distillation, *Environ. Sci. Technol.* 54 (2020) 2548–2555, https://doi.org/10.1021/ACS.EST.9B07622/ASSET/IMAGES/LARGE/ES9B07622_0004.JPEG.
- [78] Z. Cui, N.T. Hassankiadeh, Y. Zhuang, E. Drioli, Y.M. Lee, Crystalline polymorphism in poly(vinylidene fluoride) membranes, *Prog. Polym. Sci.* 51 (2015) 94–126, <https://doi.org/10.1016/J.PROGPOLYMSCI.2015.07.007>.
- [79] L. Eykens, K. De Sitter, C. Dotremont, L. Pinoy, B. Van der Bruggen, Characterization and performance evaluation of commercially available hydrophobic membranes for direct contact membrane distillation, *Desalination* 392 (2016) 63–73, <https://doi.org/10.1016/J.DESAL.2016.04.006>.
- [80] N. Thomas, M.O. Mavukkandy, S. Loutatidou, H.A. Arafat, Membrane distillation research & implementation: Lessons from the past five decades, *Sep. Purif. Technol.* 189 (2017) 108–127, <https://doi.org/10.1016/j.seppur.2017.07.069>.
- [81] H.C. Duong, D. Chuai, Y.C. Woo, H.K. Shon, L.D. Nghiem, V. Sencadas, A novel electrospun, hydrophobic, and elastomeric styrene-butadiene-styrene membrane for membrane distillation applications, *J Memb Sci* 549 (2018) 420–427, <https://doi.org/10.1016/J.MEMSCI.2017.12.024>.
- [82] Q. Huang, S. Gao, Y. Huang, M. Zhang, C. Xiao, Study on photothermal PVDF/ATO nanofiber membrane and its membrane distillation performance, *J Memb Sci* 582 (2019) 203–210, <https://doi.org/10.1016/J.MEMSCI.2019.04.019>.
- [83] A. Shaheen, S. AlBadi, B. Zhuman, H. Taher, F. Banat, F. AlMarzooqi, Photothermal air gap membrane distillation for the removal of heavy metal ions from wastewater, *Chem. Eng. J.* 431 (2022) 133909, <https://doi.org/10.1016/J.CEJ.2021.133909>.
- [84] Z. Cui, E. Drioli, Y.M. Lee, Recent progress in fluoropolymers for membranes, *Prog. Polym. Sci.* 39 (2014) 164–198, <https://doi.org/10.1016/J.PROGPOLYMSCI.2013.07.008>.
- [85] J. Zuo, T.S. Chung, G.S. O'Brien, W. Kosar, Hydrophobic/hydrophilic PVDF/Ultem® dual-layer hollow fiber membranes with enhanced mechanical properties for vacuum membrane distillation, *J Memb Sci* 523 (2017) 103–110, <https://doi.org/10.1016/J.MEMSCI.2016.09.030>.
- [86] A. Gugliuzza, E. Drioli, PVDF and HYFLON AD membranes: Ideal interfaces for contactor applications, *J Memb Sci* 300 (2007) 51–62, <https://doi.org/10.1016/J.MEMSCI.2007.05.004>.
- [87] G. Grasso, F. Galiano, M.J. Yoo, R. Mancuso, H.B. Park, B. Gabriele, A. Figoli, E. Drioli, Development of graphene-PVDF composite membranes for membrane distillation, *J Memb Sci* 604 (2020) 118017, <https://doi.org/10.1016/J.MEMSCI.2020.118017>.
- [88] M. Bhadra, S. Roy, S. Mitra, Desalination across a graphene oxide membrane via direct contact membrane distillation, *Desalination* 378 (2016) 37–43, <https://doi.org/10.1016/J.DESAL.2015.09.026>.
- [89] M. Bhadra, S. Roy, S. Mitra, A bilayered structure comprised of functionalized carbon nanotubes for desalination by membrane distillation, *ACS Appl. Mater. Interfaces* 8 (2016) 19507–19513, https://doi.org/10.1021/ACSAMI.6B05644/ASSET/IMAGES/LARGE/AM-2016-05644F_0005.JPEG.
- [90] M. Tang, D. Hou, C. Ding, K. Wang, D. Wang, J. Wang, Anti-oil-fouling hydrophobic-superoleophobic composite membranes for robust membrane distillation performance, *Sci. Total Environ.* 696 (2019) 133883, <https://doi.org/10.1016/J.SCITOTENV.2019.133883>.
- [91] L.F. Dumée, K. Sears, J. Schütz, N. Finn, C. Huynh, S. Hawkins, M. Duke, S. Gray, Characterization and evaluation of carbon nanotube Bucky-Paper membranes for direct contact membrane distillation, *J Memb Sci* 351 (2010) 36–43, <https://doi.org/10.1016/J.MEMSCI.2010.01.025>.
- [92] M.S. Fahmey, A.H.M. El-Aassar, M.M. Abo-Elfadel, A.S. Orabi, R. Das, Comparative performance evaluations of nanomaterials mixed polysulfone: a scale-up approach through vacuum enhanced direct contact membrane distillation for water desalination, *Desalination* 451 (2019) 111–116, <https://doi.org/10.1016/J.DESAL.2017.08.020>.
- [93] A. Anvari, K.M. Kekre, A. Azimi Yancheshme, Y. Yao, A. Ronen, Membrane distillation of high salinity water by induction heated thermally conducting membranes, *J Memb Sci* 589 (2019) 117253, <https://doi.org/10.1016/J.MEMSCI.2019.117253>.
- [94] M.R. Elmarghany, A.H. El-Shazly, S. Rajabzadeh, M.S. Salem, M.A. Shouman, M.N. Sabry, H. Matsuyama, N. Nady, Triple-layer nanocomposite membrane prepared by electrospinning based on modified PES with carbon nanotubes for membrane distillation applications, *Membranes* 10 (2020) 15, <https://doi.org/10.3390/MEMBRANES1001015>, 15 10 (2020).
- [95] L.D. Tijjing, Y.C. Woo, W.G. Shim, T. He, J.S. Choi, S.H. Kim, H.K. Shon, Superhydrophobic nanofiber membrane containing carbon nanotubes for high-performance direct contact membrane distillation, *J Memb Sci* 502 (2016) 158–170, <https://doi.org/10.1016/J.MEMSCI.2015.12.014>.
- [96] Z.Q. Dong, X.H. Ma, Z.L. Xu, Z.Y. Gu, Superhydrophobic modification of PVDF-SiO₂ electrospun nanofiber membranes for vacuum membrane distillation, *RSC Adv.* 5 (2015) 67962–67970, <https://doi.org/10.1039/C5RA10575G>.
- [97] Y.C. Woo, L.D. Tijjing, W.G. Shim, J.S. Choi, S.H. Kim, T. He, E. Drioli, H.K. Shon, Water desalination using graphene-enhanced electrospun nanofiber membrane via air gap membrane distillation, *J Memb Sci* 520 (2016) 99–110, <https://doi.org/10.1016/J.MEMSCI.2016.07.049>.
- [98] J. Zuo, T.S. Chung, G.S. O'Brien, W. Kosar, Hydrophobic/hydrophilic PVDF/Ultem® dual-layer hollow fiber membranes with enhanced mechanical properties for vacuum membrane distillation, *J Memb Sci* 523 (2017) 103–110, <https://doi.org/10.1016/J.MEMSCI.2016.09.030>.
- [99] J. Pan, C. Xiao, Q. Huang, H. Liu, J. Hu, ECTFE porous membranes with conveniently controlled microstructures for vacuum membrane distillation, *J Mater Chem A Mater* 3 (2015) 23549–23559, <https://doi.org/10.1039/C5TA07629C>.
- [100] D. Cheng, L. Zhao, N. Li, S.J.D. Smith, D. Wu, J. Zhang, D. Ng, C. Wu, M.R. Martinez, M.P. Batten, Z. Xie, Aluminum fumarate MOF/PVDF hollow fiber membrane for enhancement of water flux and thermal efficiency in direct contact membrane distillation, *J Memb Sci* 588 (2019) 117204, <https://doi.org/10.1016/J.MEMSCI.2019.117204>.
- [101] F. Yang, J.E. Efome, D. Rana, T. Matsuura, C. Lan, Metal-organic frameworks supported on nanofiber for desalination by direct contact membrane distillation, *ACS Appl. Mater. Interfaces* 10 (2018) 11251–11260, https://doi.org/10.1021/ACSAMI.8B01371/ASSET/IMAGES/LARGE/AM-2018-01371A_0004.JPEG.
- [102] Z. Huang, G. Yang, J. Zhang, S. Gray, Z. Xie, Dual-layer membranes with a thin film hydrophilic MOF/PVA nanocomposite for enhanced antiwetting property in membrane distillation, *Desalination* 518 (2021) 115268, <https://doi.org/10.1016/J.DESAL.2021.115268>.
- [103] M.R.S. Kebria, A. Rahimpour, G. Bakeri, R. Abedini, Experimental and theoretical investigation of thin ZIF-8/chitosan coated layer on air gap membrane distillation performance of PVDF membrane, *Desalination* 450 (2019) 21–32, <https://doi.org/10.1016/J.DESAL.2018.10.023>.
- [104] R. Zhou, D. Rana, T. Matsuura, C.Q. Lan, Effects of multi-walled carbon nanotubes (MWCNTs) and integrated MWCNTs/SiO₂ nano-additives on PVDF polymeric membranes for vacuum membrane distillation, *Sep. Purif. Technol.* 217 (2019) 154–163, <https://doi.org/10.1016/J.SEPPUR.2019.02.013>.
- [105] E.J. Lee, A.K. An, P. Hadi, S. Lee, Y.C. Woo, H.K. Shon, Advanced multi-nozzle electrospun functionalized titanium dioxide/polyvinylidene fluoride-co-hexafluoropropylene (TiO₂/PVDF-HFP) composite membranes for direct contact membrane distillation, *J Memb Sci* 524 (2017) 712–720, <https://doi.org/10.1016/J.MEMSCI.2016.11.069>.

- [106] P. Bhaskar, L.A. Bosworth, R. Wong, M.A. O'Brien, H. Kriel, E. Smit, D.A. McGrouther, J.K. Wong, S.H. Cartmell, Cell response to sterilized electrospun poly (ϵ -caprolactone) scaffolds to aid tendon regeneration in vivo, *J. Biomed. Mater. Res.* 105 (2017) 389–397, <https://doi.org/10.1002/JBM.A.35911>.
- [107] J. Drelich, E. Chibowski, Superhydrophilic and superwetting surfaces: definition and mechanisms of control, *Langmuir* 26 (2010) 18621–18623, https://doi.org/10.1021/LA1039893/ASSET/IMAGES/MEDIUM/LA-2010-039893_0002.GIF.
- [108] X. Han, W. Wang, K. Zuo, L. Chen, L. Yuan, J. Liang, Q. Li, P.M. Ajayan, Y. Zhao, J. Lou, Bio-derived ultrathin membrane for solar driven water purification, *Nano Energy* 60 (2019) 567–575, <https://doi.org/10.1016/J.NANOEN.2019.03.089>.
- [109] Y.Z. Tan, H. Wang, L. Han, M.B. Tanis-Kanbur, M.V. Pranav, J.W. Chew, Photothermal-enhanced and fouling-resistant membrane for solar-assisted membrane distillation, *J. Memb. Sci.* 565 (2018) 254–265, <https://doi.org/10.1016/J.MEMSCI.2018.08.032>.
- [110] B. Gong, H. Yang, S. Wu, J. Yan, K. Cen, Z. Bo, K.K. Ostrikov, Superstructure-enabled anti-fouling membrane for efficient photothermal distillation, *ACS Sustain. Chem. Eng.* 7 (2019) 20151–20158, https://doi.org/10.1021/ACSUSCHEMENG.9B06160/SUPPL_FILE/SC9B06160_SI_001.PDF.
- [111] D. Ghim, X. Wu, M. Suazo, Y.S. Jun, Achieving maximum recovery of latent heat in photothermally driven multi-layer stacked membrane distillation, *Nano Energy* 80 (2021) 105444, <https://doi.org/10.1016/J.NANOEN.2020.105444>.
- [112] M.U. Farid, J.A. Kharraz, A.K. An, Plasmonic titanium nitride nano-enabled membranes with high structural stability for efficient photothermal desalination, *ACS Appl. Mater. Interfaces* 13 (2021) 3805–3815, https://doi.org/10.1021/ACSAMI.0C17154/ASSET/IMAGES/LARGE/AMOC17154_0006.JPEG.
- [113] J. Huang, Y. Hu, Y. Bai, Y. He, J. Zhu, Novel solar membrane distillation enabled by a PDMS/CNT/PVDF membrane with localized heating, *Desalination* 489 (2020) 114529, <https://doi.org/10.1016/J.DESAL.2020.114529>.
- [114] Y. Zhang, K. Li, L. Liu, K. Wang, J. Xiang, D. Hou, J. Wang, Titanium nitride nanoparticle embedded membrane for photothermal membrane distillation, *Chemosphere* 256 (2020) 127053, <https://doi.org/10.1016/J.CHEMOSPHERE.2020.127053>.
- [115] W. Li, Y. Chen, L. Yao, X. Ren, Y. Li, L. Deng, Fe₃O₄/PVDF-HFP photothermal membrane with in-situ heating for sustainable, stable and efficient pilot-scale solar-driven membrane distillation, *Desalination* 478 (2020) 114288, <https://doi.org/10.1016/J.DESAL.2019.114288>.
- [116] S. Cao, X. Wu, Y. Zhu, R. Gupta, A. Tan, Z. Wang, Y.S. Jun, S. Singamaneni, Polydopamine/hydroxyapatite nanowire-based bilayered membrane for photothermal-driven membrane distillation, *J. Mater. Chem. A* Mater 8 (2020) 5147–5156, <https://doi.org/10.1039/c9ta12703h>.
- [117] M. Wu, S. Ding, L. Deng, X. Wang, PPy nanotubes-enabled in-situ heating nanofibrous composite membrane for solar-driven membrane distillation, *Sep. Purif. Technol.* 281 (2022) 119995, <https://doi.org/10.1016/J.SEPPUR.2021.119995>.
- [118] X. Wu, S. Cao, D. Ghim, Q. Jiang, S. Singamaneni, Y.S. Jun, A thermally engineered polydopamine and bacterial nanocellulose bilayer membrane for photothermal membrane distillation with bactericidal capability, *Nano Energy* 79 (2021) 105353, <https://doi.org/10.1016/J.NANOEN.2020.105353>.
- [119] D. Hegemann, H. Brunner, C. Oehr, Plasma treatment of polymers for surface and adhesion improvement, *Nucl. Instrum. Methods Phys. Res. B* 208 (2003) 281–286, [https://doi.org/10.1016/S0168-583X\(03\)00644-X](https://doi.org/10.1016/S0168-583X(03)00644-X).
- [120] C.M. Chan, T.M. Ko, H. Hiraoka, Polymer surface modification by plasmas and photons, *Surf. Sci. Rep.* 24 (1996) 1–54, [https://doi.org/10.1016/0167-5729\(96\)80003-3](https://doi.org/10.1016/0167-5729(96)80003-3).
- [121] S.S. Ray, H.K. Lee, Y.N. Kwon, Review on blueprint of designing anti-wetting polymeric membrane surfaces for enhanced membrane distillation performance, <https://doi.org/10.3390/polym12010023>, 2020.
- [122] K. Kamlangkla, B. Paosawatyanong, V. Pavarajarn, J.H. Hodak, S.K. Hodak, Mechanical strength and hydrophobicity of cotton fabric after SF₆ plasma treatment, *Appl. Surf. Sci.* 256 (2010) 5888–5897, <https://doi.org/10.1016/J.APSUSC.2010.03.070>.
- [123] X. Shen, W. Yang, Q. Zhang, Hydrophobic modification of PVDF, *Mater. Sci. Forum* 687 (2011) 658–661, <https://doi.org/10.4028/WWW.SCIENTIFIC.NET/MSF.687.658>.
- [124] R. Yang, G. Liu, X. Xu, M. Li, J. Zhang, X. Hao, Surface texture, chemistry and adsorption properties of acid blue 9 of hemp (*Cannabis sativa* L.) bast-based activated carbon fibers prepared by phosphoric acid activation, *Biomass Bioenergy* 35 (2011) 437–445, <https://doi.org/10.1016/J.BIOMBIOE.2010.08.061>.
- [125] X. Wei, B. Zhao, X.M. Li, Z. Wang, B.Q. He, T. He, B. Jiang, CF₄ plasma surface modification of asymmetric hydrophilic polyethersulfone membranes for direct contact membrane distillation, *J. Memb. Sci.* 407–408 (2012) 164–175, <https://doi.org/10.1016/J.MEMSCI.2012.03.031>.
- [126] H. Ghasemi, G. Ni, A.M. Marconnet, J. Loomis, S. Yerci, N. Miljkovic, G. Chen, Solar steam generation by heat localization, *Nat. Commun.* 5 (2014) 1–7, <https://doi.org/10.1038/ncomms5449>, 2014 5:1.
- [127] Y. Liao, R. Wang, A.G. Fane, Engineering superhydrophobic surface on poly(vinylidene fluoride) nanofiber membranes for direct contact membrane distillation, *J. Memb. Sci.* 440 (2013) 77–87, <https://doi.org/10.1016/J.MEMSCI.2013.04.006>.
- [128] P. Yimsiri, M.R. MacKley, Spin and dip coating of light-emitting polymer solutions: Matching experiment with modelling, *Chem. Eng. Sci.* 61 (2006) 3496–3505, <https://doi.org/10.1016/J.CES.2005.12.018>.
- [129] Y.X. Huang, Z. Wang, J. Jin, S. Lin, Novel Janus membrane for membrane distillation with simultaneous fouling and wetting resistance, *Environ. Sci. Technol.* 51 (2017) 13304–13310, https://doi.org/10.1021/ACS.EST.7B02848/ASSET/IMAGES/LARGE/ES-2017-02848T_0006.JPEG.
- [130] L. Dumée, J.L. Campbell, K. Sears, J. Schütz, N. Finn, M. Duke, S. Gray, The impact of hydrophobic coating on the performance of carbon nanotube bucky-paper membranes in membrane distillation, *Desalination* 283 (2011) 64–67, <https://doi.org/10.1016/J.DESAL.2011.02.046>.
- [131] Q. Jiang, H. Gholami Derami, D. Ghim, S. Cao, Y.S. Jun, S. Singamaneni, Polydopamine-filled bacterial nanocellulose as a biodegradable interfacial photothermal evaporator for highly efficient solar steam generation, *J. Mater. Chem. A* Mater 5 (2017) 18397–18402, <https://doi.org/10.1039/C7TA04834C>.
- [132] Q. He, S. Wang, S. Zeng, Z. Zheng, Experimental investigation on photothermal properties of nanofluids for direct absorption solar thermal energy systems, *Energy Convers. Manag.* 73 (2013) 150–157, <https://doi.org/10.1016/J.ENCONMAN.2013.04.019>.
- [133] Scopus - Document details - photothermal properties of nanofluid-based solar collector | Signed in, n.d. https://www.scopus.com/record/display.uri?eid=2-s2.0-85058243857&origin=inward&featureToggles=FEATURE_NEW_DOC_DETAILS_EXPORT:1. (Accessed 17 July 2022).
- [134] Z. Meng, D. Han, D. Wu, H. Zhu, Q. Li, Thermal conductivities, rheological behaviors and photothermal properties of ethylene Glycol-based nanofluids containing carbon black nanoparticles, *Procedia Eng.* 36 (2012) 521–527, <https://doi.org/10.1016/J.PROENG.2012.03.076>.
- [135] Y. Xuan, H. Duan, Q. Li, Enhancement of solar energy absorption using a plasmonic nanofluid based on TiO₂/Ag composite nanoparticles, *RSC Adv.* 4 (2014) 16206–16213, <https://doi.org/10.1039/C4RA00630E>.
- [136] P. Wang, Emerging investigator series: the rise of nano-enabled photothermal materials for water evaporation and clean water production by sunlight, *Environ. Sci.: Nano* 5 (2018) 1078–1089, <https://doi.org/10.1039/C8EN00156A>.
- [137] Y. Han, Z. Xu, C. Gao, Ultrathin graphene Nanofiltration membrane for water purification, *Adv. Funct. Mater.* 23 (2013) 3693–3700, <https://doi.org/10.1002/ADFM.201202601>.
- [138] L. Nassar, H.M. Hegab, H. Khalil, V.S. Wadi, V. Naddeo, F. Banat, S.W. Hasan, Development of green polylactic acid asymmetric ultrafiltration membranes for nutrient removal, *Sci. Total Environ.* 824 (2022) 153869, <https://doi.org/10.1016/j.scitotenv.2022.153869>.
- [139] 1. What is particulate Matter (PM)?, n.d. <https://www.greenfacts.org/en/particulate-matter-pm/level-3/01-presentation.htm#0p0>. (Accessed 13 November 2020).
- [140] S. Roy, M. Bhadra, S. Mitra, Enhanced desalination via functionalized carbon nanotube immobilized membrane in direct contact membrane distillation, *Sep. Purif. Technol.* 136 (2014) 58–65, <https://doi.org/10.1016/J.SEPPUR.2014.08.009>.
- [141] X. Hu, W. Xu, L. Zhou, Y. Tan, Y. Wang, S. Zhu, J. Zhu, Tailoring graphene oxide-based Aerogels for efficient solar steam generation under one sun, *Adv. Mater.* 29 (2017) 1604031, <https://doi.org/10.1002/ADMA.201604031>.
- [142] Y. Fu, G. Wang, T. Mei, J. Li, J. Wang, X. Wang, Accessible graphene Aerogel for efficiently harvesting solar energy, *ACS Sustain. Chem. Eng.* 5 (2017) 4665–4671, https://doi.org/10.1021/ACSUSCHEMENG.6B03207/ASSET/IMAGES/LARGE/SC-2016-03207Q_0006.JPEG.
- [143] Y. Ito, Y. Tanabe, J. Han, T. Fujita, K. Tanigaki, M. Chen, Multifunctional porous graphene for high-efficiency steam generation by heat localization, *Adv. Mater.* 27 (2015) 4302–4307, <https://doi.org/10.1002/ADMA.201501832>.
- [144] K.K. Liu, Q. Jiang, S. Tadepalli, R. Raliya, P. Biswas, R.R. Naik, S. Singamaneni, Wood-graphene oxide composite for highly efficient solar steam generation and desalination, *ACS Appl. Mater. Interfaces* 9 (2017) 7675–7681, <https://doi.org/10.1021/acsami.7b01307>.

- [145] J. Zhang, Z. Song, B. Li, Q. Wang, S. Wang, Fabrication and characterization of superhydrophobic poly (vinylidene fluoride) membrane for direct contact membrane distillation, *Desalination* 324 (2013) 1–9, <https://doi.org/10.1016/J.DESAL.2013.05.018>.
- [146] M. Umlauff, J. Hoffmann, H. Kalt, W. Langbein, J.M. Hvam, M. Scholl, J. Söllner, M. Heuken, B. Jobst, D. Hommel, Direct observation of free-exciton thermalization in quantum-well structures, *Phys. Rev. B* 57 (1998) 1390, <https://doi.org/10.1103/PhysRevB.57.1390>.
- [147] J. Wang, Y. Li, L. Deng, N. Wei, Y. Weng, S. Dong, D. Qi, J. Qiu, X. Chen, T. Wu, High-performance photothermal conversion of narrow-bandgap Ti2O3 nanoparticles, *Adv. Mater.* 29 (2017) 1603730, <https://doi.org/10.1002/ADMA.201603730>.
- [148] M. Ye, J. Jia, Z. Wu, C. Qian, R. Chen, P.G. O'Brien, W. Sun, Y. Dong, G.A. Ozin, Synthesis of black TiO₂ nanoparticles by Mg reduction of TiO₂ Nanocrystals and their application for solar water evaporation, *Adv. Energy Mater.* 7 (2017) 1601811, <https://doi.org/10.1002/AENM.201601811>.
- [149] G. Zhu, J. Xu, W. Zhao, F. Huang, Constructing black titania with unique nanocage structure for solar desalination, *ACS Appl. Mater. Interfaces* 8 (2016) 31716–31721, https://doi.org/10.1021/ACSAMI.6B11466/ASSET/IMAGES/LARGE/AM-2016-11466J_0006.JPEG.
- [150] Y. Shi, R. Li, L. Shi, E. Ahmed, Y. Jin, P. Wang, A robust CuCr2O₄/SiO₂ composite photothermal material with Underwater black property and extremely high thermal stability for solar-driven water evaporation, *Adv Sustain Syst* 2 (2018) 1700145, <https://doi.org/10.1002/ADSU.201700145>.
- [151] B.S. Lalia, E. Guillen, H.A. Arafat, R. Hashaikheh, Nanocrystalline cellulose reinforced PVDF-HFP membranes for membrane distillation application, *Desalination* 332 (2014) 134–141, <https://doi.org/10.1016/J.DESAL.2013.10.030>.
- [152] X. Li, Y. Liu, J. Wang, J. Gascon, J. Li, B. Van Der Bruggen, Metal–organic frameworks based membranes for liquid separation, *Chem. Soc. Rev.* 46 (2017) 7124–7144, <https://doi.org/10.1039/C7CS00575J>.
- [153] J. Zuo, T.-S. Chung, S. Gray, A.Y. Hoekstra, Metal–organic framework-functionalized Alumina membranes for vacuum membrane distillation, *Water* 8 (2016) 586, <https://doi.org/10.3390/W8120586>, 586 8 (2016).
- [154] Z. Deng, J. Zhou, L. Miao, C. Liu, Y. Peng, L. Sun, S. Tanemura, The emergence of solar thermal utilization: solar-driven steam generation, *J Mater Chem A Mater* 5 (2017) 7691–7709, <https://doi.org/10.1039/C7TA01361B>.
- [155] H. Chen, L. Shao, Q. Li, J. Wang, Gold nanorods and their plasmonic properties, *Chem. Soc. Rev.* 42 (2013) 2679–2724, <https://doi.org/10.1039/C2CS35367A>.
- [156] S. Loeb, C. Li, J.H. Kim, Solar photothermal Disinfection using broadband-light absorbing gold nanoparticles and carbon black, *Environ. Sci. Technol.* 52 (2018) 205–213, https://doi.org/10.1021/ACS.EST.7B04442/ASSET/IMAGES/LARGE/ES-2017-04442K_0007.JPEG.
- [157] K. Bae, G. Kang, S.K. Cho, W. Park, K. Kim, W.J. Padilla, Flexible thin-film black gold membranes with ultrabroadband plasmonic nanofocusing for efficient solar vapour generation, *Nat. Commun.* 6 (2015) 1–9, <https://doi.org/10.1038/ncomms10103>, 1 6 (2015).
- [158] L. Zhou, Y. Tan, J. Wang, W. Xu, Y. Yuan, W. Cai, S. Zhu, J. Zhu, 3D self-assembly of aluminium nanoparticles for plasmon-enhanced solar desalination, *Nat. Photonics* 10 (2016) 393–398, <https://doi.org/10.1038/nphoton.2016.75>, 6 10 (2016).
- [159] M. Zhu, Y. Li, F. Chen, X. Zhu, J. Dai, Y. Li, Z. Yang, X. Yan, J. Song, Y. Wang, E. Hitz, W. Luo, M. Lu, B. Yang, L. Hu, Plasmonic wood for high-efficiency solar steam generation, *Adv. Energy Mater.* 8 (2018) 1701028, <https://doi.org/10.1002/AENM.201701028>.
- [160] W. Li, Y. Chen, L. Yao, X. Ren, Y. Li, L. Deng, Fe3O₄/PVDF-HFP photothermal membrane with in-situ heating for sustainable, stable and efficient pilot-scale solar-driven membrane distillation, *Desalination* 478 (2020) 114288, <https://doi.org/10.1016/J.DESAL.2019.114288>.
- [161] P.D. Dongare, A. Alabastri, S. Pedersen, K.R. Zodrow, N.J. Hogan, O. Neumann, J. Wud, T. Wang, A. Deshmukh, M. Elimelech, Q. Li, P. Nordlander, N.J. Halas, Nanophotonics-enabled solar membrane distillation for off-grid water purification, *Proc Natl Acad Sci U S A* 114 (2017) 6936–6941, <https://doi.org/10.1073/PNAS.1701835114>.
- [162] P. Wang, Emerging investigator series: the rise of nano-enabled photothermal materials for water evaporation and clean water production by sunlight, *Environ. Sci.: Nano* 5 (2018) 1078–1089, <https://doi.org/10.1039/C8EN00156A>.
- [163] Y.R. Chen, R. Xin, X. Huang, K. Zuo, K.L. Tung, Q. Li, Wetting-resistant photothermal nanocomposite membranes for direct solar membrane distillation, *J Membr Sci* 620 (2021) 118913, <https://doi.org/10.1016/J.MEMSCI.2020.118913>.
- [164] D. Rice, S.J. Ghadimi, A.C. Barrios, S. Henry, W.S. Walker, Q. Li, F. Perreault, Scaling resistance in Nanophotonics-enabled solar membrane distillation, *Environ. Sci. Technol.* 54 (2020) 2548–2555, https://doi.org/10.1021/ACS.EST.9B07622/ASSET/IMAGES/LARGE/ES9B07622_0004.JPEG.
- [165] X. Wu, Q. Jiang, D. Ghim, S. Singamaneni, Y.S. Jun, Localized heating with a photothermal polydopamine coating facilitates a novel membrane distillation process, *J Mater Chem A Mater* 6 (2018) 18799–18807, <https://doi.org/10.1039/C8TA05738A>.
- [166] J. Huang, Y. Hu, Y. Bai, Y. He, J. Zhu, Solar membrane distillation enhancement through thermal concentration, *Energy* 211 (2020) 118720, <https://doi.org/10.1016/J.ENERGY.2020.118720>.
- [167] A. Boubakri, A. Hafiane, S.A.T. Bouguecha, Direct contact membrane distillation: capability to desalt raw water, *Arab. J. Chem.* 10 (2017) S3475–S3481, <https://doi.org/10.1016/J.ARABJC.2014.02.010>.
- [168] P.D. Dongare, A. Alabastri, S. Pedersen, K.R. Zodrow, N.J. Hogan, O. Neumann, J. Wud, T. Wang, A. Deshmukh, M. Elimelech, Q. Li, P. Nordlander, N.J. Halas, Nanophotonics-enabled solar membrane distillation for off-grid water purification, *Proc Natl Acad Sci U S A* 114 (2017) 6936–6941, <https://doi.org/10.1073/PNAS.1701835114>.
- [169] A. Siefan, E. Rachid, N. Elashwah, F. AlMarzooqi, F. Banat, R. van der Merwe, Desalination via solar membrane distillation and conventional membrane distillation: life cycle assessment case study in Jordan, *Desalination* 522 (2022) 115383, <https://doi.org/10.1016/J.DESAL.2021.115383>.
- [170] Solar desalination using membrane distillation : technical evaluation case study, n.d. <http://kth.diva-portal.org/smash/record.jsf?pid=diva2%3A739659&dswid=9782>. (Accessed 14 July 2022).
- [171] Economic evaluation of desalination by small-scale autonomous solar-powered membrane distillation units, n.d. <https://www.lenntech.com/abstracts/2199/economic-evaluation-of-desalination-by-small-scale-autonomous-solar-powered-membrane-distillation-units.html>. (Accessed 14 July 2022).
- [172] R.B. Saffarini, E.K. Summers, H.A. Arafat, J.H. Lienhard V, Economic evaluation of stand-alone solar powered membrane distillation systems, *Desalination* 299 (2012) 55–62, <https://doi.org/10.1016/J.DESAL.2012.05.017>.
- [173] E. Guillén-Burrieza, D.C. Alarcón-Padilla, P. Palenzuela, G. Zaragoza, Techno-economic assessment of a pilot-scale plant for solar desalination based on existing plate and frame MD technology, *Desalination* 374 (2015) 70–80, <https://doi.org/10.1016/J.DESAL.2015.07.014>.
- [174] M.I. Soomro, W.S. Kim, Performance and economic investigations of solar power tower plant integrated with direct contact membrane distillation system, *Energy Convers. Manag.* 174 (2018) 626–638, <https://doi.org/10.1016/J.ENCONMAN.2018.08.056>.
- [175] S.E. Moore, S.D. Mirchandani, V. Karanikola, T.M. Nenoff, R.G. Arnold, A.E. Sáez, Process modeling for economic optimization of a solar driven sweeping gas membrane distillation desalination system. <https://doi.org/10.1016/j.desal.2018.03.005>, 2018.
- [176] V. Karanikola, S.E. Moore, A. Deshmukh, R.G. Arnold, M. Elimelech, A.E. Sáez, Economic performance of membrane distillation configurations in optimal solar thermal desalination systems. <https://doi.org/10.1016/j.desal.2019.114164>, 2019.
- [177] G. Li, L. Lu, Modeling and performance analysis of a fully solar-powered stand-alone sweeping gas membrane distillation desalination system for island and coastal households. <https://doi.org/10.1016/j.enconman.2019.112375>, 2019.
- [178] N.A.S. Elminshawy, M.A. Gadalla, M. Bassiouni, K. El-Nahhas, A. Elminshawy, Y. Elhenawy, A novel concentrated photovoltaic-driven membrane distillation hybrid system for the simultaneous production of electricity and potable water, *Zewail City of Science and Technology* (1257). <https://doi.org/10.1016/j.renene.2020.08.041>.
- [179] M.M. Alquraish, S. Mejri, K.A. Abuhasel, K. Zhani, Experimental investigation of a pilot solar-assisted permeate gap membrane distillation, *Membranes* 11 (2021) 336, <https://doi.org/10.3390/MEMBRANES11050336>, 336 11 (2021).
- [180] Y.H. Chen, H.G. Hung, C.D. Ho, H. Chang, Economic design of solar-driven membrane distillation systems for desalination, *Membranes* 11 (2021) 1–20, <https://doi.org/10.3390/MEMBRANES11010015>.
- [181] J. Choi, J. Cho, J. Shin, H. Cha, J. Jung, K.G. Song, Performance and economic analysis of a solar membrane distillation pilot plant under various operating conditions, *Energy Convers. Manag.* 268 (2022) 115991, <https://doi.org/10.1016/J.ENCONMAN.2022.115991>.
- [182] A. Hafiz Al Hariri, A.E. Khalifa, S.M. Alawad, Techno-economic analysis of solar-powered membrane distillation system with circulated permeate gap, *Sol. Energy* 267 (2024) 112243, <https://doi.org/10.1016/J.SOLENER.2023.112243>.

- [183] N. Ghaffour, T.M. Missimer, G.L. Amy, Technical review and evaluation of the economics of water desalination: current and future challenges for better water supply sustainability, *Desalination* 309 (2013) 197–207, <https://doi.org/10.1016/J.DESAL.2012.10.015>.
- [184] S. Al-Obaidani, E. Curcio, F. Macedonio, G. Di Profio, H. Al-Hinai, E. Drioli, Potential of membrane distillation in seawater desalination: thermal efficiency, sensitivity study and cost estimation, *J Memb Sci* 323 (2008) 85–98, <https://doi.org/10.1016/J.MEMSCI.2008.06.006>.
- [185] C. Yong, Economic analysis of desalination technologies in the context of carbon pricing, and opportunities for membrane distillation) Economic analysis of desalination technologies in the context of carbon pricing, and opportunities for membrane distillation, 1873–4464, <http://ac.els-cdn.com/>, 2013. (Accessed 22 March 2024).
- [186] Z. Wang, T. Horseman, A.P. Straub, N.Y. Yip, D. Li, M. Elimelech, S. Lin, Pathways and challenges for efficient solar-thermal desalination, *Sci. Adv.* 5 (2019), https://doi.org/10.1126/SCIADV.AAX0763/SUPPL_FILE/AAX0763_SM.PDF.
- [187] A. Al-Karaghoul, L.L. Kazmerski, Energy consumption and water production cost of conventional and renewable-energy-powered desalination processes, *Renew. Sustain. Energy Rev.* 24 (2013) 343–356, <https://doi.org/10.1016/J.RSER.2012.12.064>.